AB INITIO CALCULATIONS OF LIGHT HYPERNUCLEI

THIRI YADANAR HTUN

A Thesis Submitted in Partial Fulfillment of the Requirements for the

Degree of Doctor of Philosophy in Physics

Suranaree University of Technology

Academic Year 2021

การศึกษาไฮเปอร์นิวคลีไอแบบเบาด้วยการคำนวณแบบ แอบ อินิธิโอ

นางสาวติริ ญาดาณาร์ ทุน

วิทยานิพนธ์นี้เป็นส่วนหนึ่งของการศึกษาตามหลักสูตรปริญญาวิทยาศาสตรดุษฎีบัณฑิต
สาขาวิชาฟิสิกส์
มหาวิทยาลัยเทคโนโลยีสุรนารี
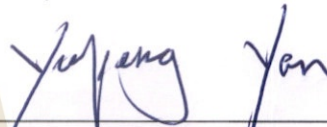ปีการศึกษา 2564

AB INITIO CALCULATIONS OF LIGHT HYPERNUCLEI

Suranaree University of Technology has approved this thesis submitted in partial fulfillment of the requirements for the Degree of Doctor of Philosophy.

Thesis Examining Committee

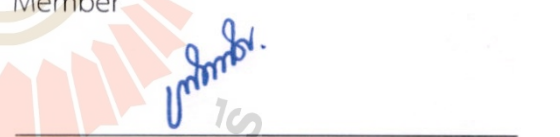_____
(Assoc. Prof. Dr. Panomsak Meemon)

Chairperson

_____
(Prof. Dr. Yupeng Yan)

Member (Thesis Advisor)

_____
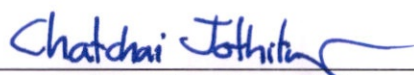(Asst. Prof. Dr. Ayut Limphirat)

Member

_____
(Asst. Prof. Dr. Khanchai Khosonthongkee)

Member

_____
(Asst. Prof. Dr. Daris Samart)

Member

_____
(Assoc. Prof. Dr. Chatchai Jothityangkoon)

Vice Rector for Academic Affairs

and Quality Assurance

_____
(Prof. Dr. Santi Maensiri)

Dean of Institute of Science

ติริ ญาดาณาร์ ทุน : การศึกษาไฮเปอร์นิวคลีไอแบบเบาด้วยการคำนวณแบบ แอบ อินิธิโอ (AB INITIO CALCULATIONS OF LIGHT HYPERNUCLEI) อาจารย์ที่ปรึกษา : ศาสตราจารย์ ดร.ยูเป็ง แยน, 64 หน้า

คำสำคัญ: ทฤษฎีสนามยังผลไครอล, แบบจำลองไร้เปลือก, วิธีการฮาร์มอนิกทรงกลม, ความไม่แน่นอนของแบบจำลอง, ไฮเปอร์นิวคลีไอแบบเปลือกเอส

พลังงานยึดเหนี่ยวสำหรับไฮเปอร์นิวคลีไอแบบเปลือกเอส อาทิ $_\Lambda^3 H$, $_\Lambda^4 H$, $_\Lambda^4 He$ และระบบ Λnn ได้ถูกคำนวณภายใต้แบบจำลองไฮเปอร์นิวเคลียร์แบบ แอบ อินิธิโอ ชนิดไร้เปลือก ซึ่งประกอบด้วยอันตรกิริยาเหมือนจริงจากทฤษฎีสนามยังผลไครอล โดยเฉพาะอย่างยิ่ง อันตรกิริยาระหว่างนิวคลีออน-นิวคลีออนที่เป็นไปได้หลายรูปแบบได้ถูกนำมาพิจารณา เพื่อบ่งชี้ความแม่นยำเชิงทฤษฎีของปริมาณไฮเปอร์นิวเคลียร์สังเกตได้อันเนื่องมาจากความไม่แน่นอนเชิงฟิสิกส์นิวเคลียร์ การคำนวณแบบสามวัตถุและแบบสี่วัตถุได้ถูกดำเนินการโดยอาศัยฐานฮาร์มอนิกแบบกวัดแกว่งในระบบจาโคบีแบบสัมพัทธ์นอกจากนี้ สูตรแก้แบบอินฟราเรดได้ถูกนำมาใช้เพื่อคาดการณ์ผลลัพธ์ในปริภูมิแบบจำลองอนันต์โดยอาศัยผลลัพธ์จากแบบจำลองไฮเปอร์นิวเคลียร์แอบ อินิธิโอ ชนิดไร้เปลือกเป็นบรรทัดฐาน นอกจากนี้ ปริมาณสังเกตได้ของสถานะกักขังสามารถนำมาใช้ในการปรับวัดเพื่อจำกัดอันตรกิริยาแบบ YN เพื่อค้นหาเรโซแนนซ์ Λnn ได้ โดยใช้ความไวขนาดเล็กของพลังงานยึดเหนี่ยวที่ได้รับการทำนายจนถึงความไม่แน่นอนเชิงฟิสิกส์นิวเคลียร์ที่ได้ค้นพบเป็นรากฐาน การคำนวณด้วยแบบจำลองไฮเปอร์นิวเคลียร์แบบ แอบอินิธิโอ ชนิดไร้เปลือกได้รับการขยายไปยังสถานะต่อเนื่องโดยใช้วิธีการเมทริกซ์แบบเจพร้อมด้วยฐานกวัดแกว่งทรงกลม จากการศึกษาพบว่า สถานะกักขัง Λnn ไม่มีอยู่ แต่ทำนายการมีอยู่ของสถานะเรโซแนนซ์ Λnn ที่พลังงานต่ำ

สาขาวิชาฟิสิกส์
ปีการศึกษา 2564

ลายมือชื่อนักศึกษา _____
ลายมือชื่ออาจารย์ที่ปรึกษา _____
ลายมือชื่ออาจารย์ที่ปรึกษาร่วม _____
ลายมือชื่ออาจารย์ที่ปรึกษาร่วม _____

THIRI YADANAR HTUN : AB INITIO CALCULATIONS OF LIGHT HYPERNUCLEI.

THESIS ADVISOR : PROF. YUPENG YAN, Ph.D. 64 PP.

We compute the binding energies of the s-shell hypernuclei such as $^{3}_{\Lambda}H$, $^{4}_{\Lambda}H$, $^{4}_{\Lambda}He$ and a Λnn system using the ab initio hypernuclear no-core shell model (NCSM) with realistic interactions derived from chiral effective field theory. In particular, we employ a large family of nucleon–nucleon interactions with the aim to quantify the theoretical precision of predicted hypernuclear observables arising from nuclear-physics uncertainties. The three- and four-body calculations are performed in a relative Jacobi-coordinate harmonic oscillator basis and we implement infrared correction formulas to extrapolate the NCSM results to infinite model space. Based on our finding of small sensitivity of the predicted binding energies to nuclear-physics uncertainties, these bound-state observables can be used in the calibration procedure to constrain the YN interactions. In searching for Λnn resonances, we extend the NCSM calculation to the continuum state by employing the J-matrix formalism using the hyperspherical oscillator basis. The calculations show that no Λnn bound state exists, but predict a low-lying Λnn resonant state.

School of Physics

Academic Year 2021

Student's Signature _____

Advisor's Signature _____

Co-Advisor's Signature _____

Co-Advisor's Signature _____

ACKNOWLEDGEMENTS

CONTENTS

CONTENTS (Continued)

LIST OF TABLES

LIST OF FIGURES

LIST OF FIGURES (Continued)

LIST OF ABBREVIATIONS

NCSM   No-Core Shell Model

χEFT   Chiral Effective Field Theory

SS-HORSE   Single State Harmonic Oscillator Representation of
            Scattering Equations

HH   Hyperspherical Harmonic

HO   Harmonic Oscillator
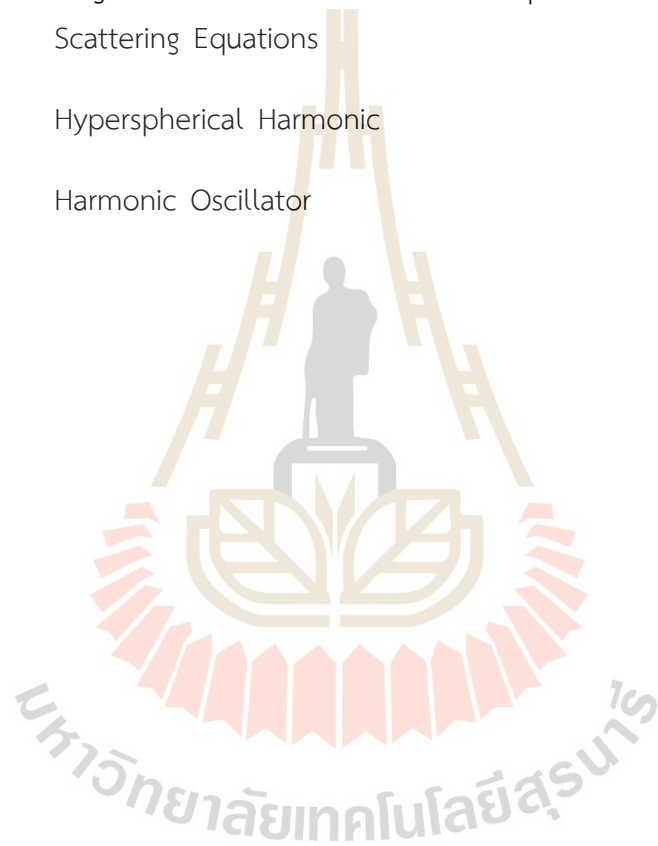
CHAPTER I

INTRODUCTION

The study of hypernuclei is very important to understand the hyperon–nucleon interactions. Unlike the nucleon–nucleon (NN) case, the hyperon–nucleon (YN) scattering experiments are quite difficult to carry out due to the hyperons' short lifetime. YN scattering data are very limited to fully determine the YN interactions. Fortunately, the existing data of few-body hypernuclei such as the Λ-binding energies and excitation spectra could provide the important constrain on YN interaction (Davis, 2005). However, it is a very challenging task to apply the precise experimental hypernuclear data in order to constrain the hyperon-nucleon interactions.

First, the modern *ab initio* methods without uncontrolled approximations to renormalize the YN interactions developed in the recent past (Nogga, 2013; Lonardoni et al., 2013; Wirth et al., 2014; Wirth et al., 2018; Contessi et al., 2018; Le et al., 2020; Schäfer et al., 2021). Second, it is very important to understand all sources of uncertainties including in the process of going from a chiral NN (YN) interaction to computed many-body nuclear (hypernuclear) observable. Uncertainty quantification is essential not only to generate the new knowledge in the nuclear and hypernuclear structure but also to obtain more new observables in order to constrain the hyperon-nucleon (YN) interaction. In the nucleon-nucleon (NN) sector, there has been significant progress in the analysis of different uncertainties in NN interactions using various methods (Furnstahl et al., 2015; Ekström et al., 2015; Carlsson et al., 2016; Pérez et al., 2015; Carlsson et al., 2016; Binder et al., 2016; Navarro Pérez et al., 2015; Acharya et al., 2016). Theoretical uncertainties such as the model error of nuclear interaction in χEFT due to the omitted size of low impact contributions in momentum expansion and the method errors due to the application of many-body method containing approximations are increasingly acknowledged. The effect on other nuclear observables was studied by propagating the well qualified uncertainties of NN interactions (Carlsson et al., 2016; Ekström et al., 2015; Navarro Pérez et al., 2015; Acharya et al., 2016). In *ab initio* hypernuclear calculations, the dominant uncertainty come from the hypernuclear

Hamiltonian which is constructed from different nuclear and hypernuclear models. The uncertainty of YN interaction is much larger than that of NN interaction due to the very limited YN scattering data. It is hard to quantify the theoretical uncertainties in YN interaction as in NN case. If the remaining freedom in the construction of realistic nuclear interactions is taken into hypernuclear calculations, it would be possible to provide more observables as the important constrains on YN interactions by studying the dependence of predicted hypernuclear bound observables on the uncertainties of NN interaction.

In this work, we are able to quantify the systematic nuclear model uncertainties in the s-shell hypernuclei such as ${}^{3}_{\Lambda}H$, ${}^{4}_{\Lambda}H$ and ${}^{4}_{\Lambda}He$. This knowledge is very important to apply these observables as important constrains on YN interactions in future calculations. Particularly, hypernuclear no-core shell model (NCSM) calculations are performed in relative Jacobi-coordinate harmonic oscillator (HO) basis by using chiral NNLO$_{\text{sim}}$ family of NN interactions and a fixed YN interaction. We study the convergence properties and the dependence on the model-space parameters. We apply the standard infrared (IR) extrapolation technique (Wendt et al., 2015) to extrapolate the NCSM results obtained in finite model spaces to infinite model space. We then present the ground- and excited state energy of our computed s-shell hypernuclei and discuss the effects of nuclear model uncertainty on hypernuclear observables. This study opens up the opportunity to quantify the uncertainty of other hypernuclear observables.

Furthermore, we analysis the Λnn bound state problem using the no-core shell model technique since the theoretical calculations for the Λnn system has been a long time as a serious doubtful bound state problem (Belyaev et al., 2008; Afnan and Gibson, 2015; Garcilazo and Valcarce, 2014; Kamada et al., 2016; Gibson and Afnan, 2019; Downs and Dalitz, 1959; Ando et al., 2015; Hildenbrand and Hammer, 2019; Schäfer et al., 2021). The calculation of Λnn system $(J^{\pi} = 1/2^{+}, T = 1)$ is carried out in Jacobi coordinate HO basis using the NN and YN interactions derived from chiral effective field model. In the extension into the continuum state, we apply the SS-HORSE (Mazur et al., 2017; Shirokov et al., 2016a; Blokhintsev et al., 2017; Lurie and Shirokov, 2004; Shirokov et al., 2018; Mazur et al., 2019) formalism, which is a single state harmonic oscillator representation of scattering equations, to calculate the low-energy phase shifts and scattering amplitude at the NCSM eigenenergies by employing hyperspherical harmonic oscil-

lator basis. The low-lying Λnn resonance energy and width are extracted from the scattering amplitude parametrization. The NCSM-SS-HORSE method (Shirokov et al., 2016b) has been successfully applied to study tetraneutron unbound system considered as true four-body scatterings. Here we first apply this method to study the three-body system with strangeness.

In the thesis, we briefly present the formalism of the hypernuclear no-core shell model and IR extrapolation technique to estimate the infinite energies in Chapter II. The study of convergence properties and uncertainty quantification for the relevant hypernuclei is presented in Chapter III. The Chapter IV presents the SS-HORSE method formalism and its application to the calculating democratic three-body decays within the NCSM as well as parametrization of scattering amplitude to extract the resonance energy and level width of Λnn system. A summary is presented in Sec. V.

CHAPTER II

HYPERNUCLEAR NO-CORE SHELL MODEL

The hypernuclear no-core shell model describes the many-body systems containing nucleons and hyperons in the HO basis where all A fermions of the system are treated as being active. The main feature of NCSM is the use of HO basis which permits one to represent the full complexity of nuclear and hypernuclear interactions efficiently with the aim to solve full A-body problems without making any approximations regarding the structure of the many-body wavefunction.

The ambition is to solve the A-body non-relativistic Schrodinger equation

$$H_A \Psi^A = E_A \Psi^A,$$ (2.1)

with realistic NN and YN interactions. The Hamiltonian matrix in many-body basis grows rapidly with the number of particles in the system and model space truncation in HO basis and the eigenvalue problem converges slowly in some cases. To solve this many-body problem, Lanczos diagonalization method is used in modern NCSM calculations to find the relevant eigenenergies and eigenstates of hypernuclear systems under our consideration.

2.1 Hypernuclear Hamiltonian and Jacobi Coordinates

The hypernuclear NCSM approach starts with the non-relativistic Hamiltonian of a hypernuclear system employing realistic two-body NN, YN interactions and realistic three-body NNN interactions

$$H = \sum_{i=1}^{A} \frac{\hbar^2}{2m_i} \vec{\nabla}_i^2 + \sum_{i<j=1}^{A-1} V_{NN}(\vec{r}_i, \vec{r}_j) + \sum_{i=1}^{A-1} V_{YN}(\vec{r}_i, \vec{r}_A)$$

$$+ \sum_{i<j<k=1}^{A-1} V_{NNN}(\vec{r}_i, \vec{r}_j, \vec{r}_k) + \Delta M,$$ (2.2)

where the mass m_i and coordinates $\vec{r}_i$ correspond to the nucleons for $i \leq A-1$ and for $i = A$ to a hyperon.

The $\Lambda N \leftrightarrow \Sigma N$ mixing effect in V_{YN} (Polinder et al., 2006) is explicitly taken into account. The mass term

$$\Delta M = \sum_i m_i - M_0, \tag{2.3}$$

is the rest-mass difference of Λ and Σ hyperons. M_0 is the total rest mass of constituent fermions in a system. The mass difference between the Λ and Σ hyperons is small, $m_\Sigma - m_\Lambda \sim 77$ MeV/c^2, compared to that of the nucleon and Δ isobar, $m_\Delta - m_N \sim 290$ MeV/c^2. This condition causes the effect of the $\Lambda N - \Sigma N$ coupling essential in the hypernuclear structure calculation. The inclusion of the coupling effect may increase the $\Lambda \Sigma$ attraction only for hypernuclear systems with non-zero isospin due to the isospin conservation. We use the isospin averaged particle masses in hypernuclear calculations (Wirth et al., 2018) and consider the full coupled channels.

The formulation of NCSM uses a translationally invariant HO basis to omit the center of mass (c.m.) coordinate. Employing Jacobi coordinates to construct the HO basis is appropriate only for $A \leq 6$ hypernuclear systems. The Jacobi coordinates can be introduced as an orthogonal transformation of the single-nucleon coordinates. There are several different sets of Jacobi coordinates that are related to each other by orthogonal transformations. In the construction of the A-body HO basis state to evaluate the two-body and three-body interaction matrix elements, in general, we need three sets of Jacobi coordinates. For our purpose, the first set of Jacobi coordinates in terms of scaled version of single-particle coordinates $\vec{x}_i = \sqrt{m_i}\,\vec{r}_i$ is defined as

$$\vec{\xi}_0 = \frac{1}{M_{1,A}} \sum_{i=1}^{A} \sqrt{m_i}\,\vec{x}_i,$$

$$\vec{\xi}_i = \sqrt{\frac{M_{1,i}m_{i+1}}{M_{1,i+1}}} \left(\frac{1}{M_{1,i}} \sum_{j=1}^{i} \sqrt{m_j}\,\vec{x}_j - \frac{1}{\sqrt{m_{i+1}}}\vec{x}_{i+1} \right). \tag{2.4}$$

The total mass of the system is $M_{kl} = \sum_{j=k}^{l} m_j$ with $i = 1, ..., A-1$. This set is employed for the construction of the antisymmetrized HO basis state of

nucleon clusters. $\vec{\xi}_0$ corresponds to the center of mass of the A-baryon system. The coordinate $\vec{\xi}_{A-1}$ corresponds to the relative coordinate between A^{th} hyperon and the c.m. coordinate of the (A-1) nucleons cluster. When two-body hyperon-nucleon interaction matrix elements need to be calculated, another set of Jacobi coordinate appropriate for the basis expansion is obtained by keeping $\vec{\xi}_0, ..., \vec{\xi}_{A-3}$ and proposing two new variables

$$
\vec{\eta}_{A-2} = \sqrt{\frac{M_{1,A-2}M_{A-1,A}}{M_{1,A}}}
$$

$$
\times \left(\frac{1}{M_{1,A-2}} \sum_{i=2}^{A-2} \sqrt{m_i}\vec{x}_i - \frac{1}{M_{A-1,A}} \sum_{i=A-1}^{A} \sqrt{m_i}\vec{x}_i \right), \qquad (2.5)
$$

$$
\vec{\eta}_{A-1} = \sqrt{\frac{m_{A-1}m_A}{M_{A-1,A}}} \left(\frac{1}{m_{A-1}}\vec{x}_{A-1} - \frac{1}{\sqrt{m_A}}\vec{x}_A \right).
$$

In order to calculate the three-body nuclear interaction matrix elements, a suitable set of Jacobi coordinate is obtained by keeping $\vec{\xi}_0, ..., \vec{\xi}_{A-4}$ and $\vec{\eta}_{A-1}$ from the previous set and introducing other two different variables

$$
\vec{\zeta}_{A-2} = \sqrt{\frac{M_{1,A-4}M_{A-3,A-1}}{M_{1,A-1}}}
$$

$$
\times \left(\frac{1}{M_{1,A-4}} \sum_{i=2}^{A-4} \sqrt{m_i}\vec{x}_i - \frac{1}{M_{A-3,A-1}} \sum_{i=A-3}^{A-1} \sqrt{m_i}\vec{x}_i \right), \qquad (2.6)
$$

$$
\vec{\zeta}_{A-3} = \sqrt{\frac{m_{A-3}M_{A-2,A-1}}{M_{A-3,A-1}}} \left(\frac{1}{m_{A-3}}\vec{x}_{A-3} - \frac{1}{M_{A-2,A-1}} \sum_{i=A-2}^{A-1} \sqrt{m_i}\vec{x}_i \right).
$$

The two-and three-body interactions in the Hamiltonian (2.2) depend only on the relative coordinates (and relative momenta) and can be represented as a potential matrix in a partial-wave decomposed relative-momentum basis $|q\gamma\rangle$, where $|\gamma\rangle \equiv |(LS)JM\chi_i\rangle$ assembling the relative quantum numbers for angular momentum, spin, total angular momentum, isospin of the involved particles in the system. When we employ the two- and three-body interactions in the NCSM

calculations, the relative momentum-space matrix elements of potential need to be transformed to a HO basis $|n\gamma\rangle \equiv |n(LS)JM\chi_i\rangle$, where n is the radial quantum number. The antisymmetrization procedure using HO basis for three- and four-body hypernuclei is presented in the Appendix A. The antisymmetrization of relative-momentum states can also be obtained by using the same procedure. The relative-momentum basis is transformed into the HO basis

$$|n\gamma\rangle = \int dq\ q^2\ |q\gamma\rangle\ \langle q\gamma|n\gamma\rangle \quad \int dq\ q^2 \phi_n^\gamma(q)\ |q\gamma\rangle\,, \tag{2.7}$$

with the momentum-space wavefunction of the HO states

$$\phi_n^\gamma(q) = (-1)^n \sqrt{\frac{2a_{\chi_i}^3 n!}{\Gamma(n+L+\frac{3}{2})}} e^{-\frac{1}{2}\rho^2}\rho^L L_n^{L+\frac{1}{2}}(\rho^2), \tag{2.8}$$

where $a_{\chi_i} = \dfrac{1}{\sqrt{\mu_{\chi_i}\Omega}}$ is the oscillator length, Ω is the oscillator frequency, $\rho = a_{\chi_i}q$ is the dimensionless relative momentum and $L_n^m(x)$ is an associated Laguerre polynomial.

2.2 Potential Models

In our calculations, we use the leading-order (LO) Bonn–Jülich SU(3)-based χEFT YN model (Polinder et al., 2006) and the next-to-next-to-leading-order (NNLO) chiral NN+NNN interactions (Carlsson et al., 2016). Renormalization is not applied to both nuclear and hypernuclear interactions. We present a brief description of the potentials that have been used in the calculations of the binding energy for light hypernuclei.

2.2.1 Nucleon-Nucleon Potentials

With the power counting fixed, B. D. CARLSSON et al. (Carlsson et al., 2016) constructed the chiral interactions from the terms or diagrams depending on the order ν and on the type of the exchanged particles. It consist of the contact interaction (V_{ct}) which is a general parametrization of the short-range physics and the pion exchanges ($V_{1\pi}, V_{2\pi}, V_{3\pi}$ and so on) which comprise the long-range part of the nuclear interactions. Each term in contact interaction is proportional to a

low-energy constant (LEC). The interactions at different orders are

$$V_{LO} = V_{ct}^{(0)} + V_{1\pi}^{(0)},$$

$$V_{NLO} = V_{LO} + V_{ct}^{(2)} + V_{1\pi}^{(2)} + V_{2\pi}^{(2)}, \tag{2.9}$$

$$V_{NNLO} = V_{NLO} + V_{1\pi}^{(3)} + V_{2\pi}^{(3)} + V_{NNN},$$

where the superscript specifies the orders ν of the interaction terms. The next to next to leading order (NNLO) NN interactions were constructed from all terms with orders $\nu \leq 3$. All 26 LECs up to a NNLO order in χEFT were optimized at the same time with respect to NN and πN scattering data as well as experimentally determined nuclear bound-state observables: $^{2,3}H$ and ^{3}He.

2.2.2 Hyperon-Nucleon Potentials

Analogous to the chiral NN potential, the YN interaction in a chiral effective field theory approach constructed by Polinder et al. (Polinder et al., 2006) based on a modified Weinberg powercounting. The limited accuracy and incompleteness of the YN scattering data do not allow for a unique partial wave analysis as in NN case. The parameters of the LO YN interaction in χEFT were directly fitted to the cross sections. The YN potential in leading order consists of nonderivative four-baryon contact term and one-pseudoscalar-meson exchange (OPME) related via $SU(3)_f$ symmetry,

$$V_{LO} = V_{ct}^{(0)} + V_{OPME}^{(0)}. \tag{2.10}$$

The leading order YN contact term potential is

$$V_{ct}^{(0)} = C_S^{BB} + C_T^{BB}\sigma_1.\sigma_2, \tag{2.11}$$

including $C_{S,T}^{\Lambda\Lambda}, C_{S,T}^{\Lambda\Sigma}$ and $C_{S,T}^{\Sigma\Sigma}$ for singlet and triplet state. There are only 5 LECs in the contact terms which were determined by a fit to only the set of 35 low-energy YN scattering data. The reasonable YN scattering data were reproduced well in the regulator cutoff range between 550 and 700 MeV.

2.3   Jacobi-Coordinate Formulation

The NCSM is based on an expansion of the total wavefunction in many-body HO basis. The Jacobi coordinate is more convenient to use in the construction of the basis state for light hypernuclei only. It is hard to build up an antisymmetrized set of nuclear HO states using relative Jacobi coordinates when the number of particles increases. The relative Jacobi coordinate HO basis allows us to carry out the calculations in larger model spaces. Since J-formulation uses the translational invariant Hamiltonian, the center of mass motion, related with $\vec{\xi_0}$, can be removed to reduce the basis states dimension. Then, a JT-coupled HO basis depending on the relative coordinates ξ_i with $i = 1, ..., A-1$, is built as

$$\left| (...(\alpha_1, \alpha_2), J_3 T_3, \alpha_3) J_4 T_4, ..., \alpha_{A-1}) JT \right\rangle , \qquad (2.12)$$

where $\alpha_i \equiv \left| n_i (l_i s_i) j_i t_i \right\rangle$ are the relative HO basis including radial, orbital, spin and isospin quantum numbers. The parentheses in Eq. (2.12) express the coupling of angular momentum and isospin. The J and T quantum numbers are the total angular momentum and total isospin of our consideration system. The state of the two-nucleon subsystem is labeled here with α_1.

For practical calculations, the basis state is truncated to a finite model space by restricting a maximum number of HO quanta N_{max}^{tot},

$$\sum_{i=1}^{A-1} (2n_i + l_i) \leq N_{max} + N_0 \equiv N_{max}^{tot}, \qquad (2.13)$$

where N_{max} is the maximum number of excitation quanta defining the many-body NCSM basis space. In our calculations for s-shell hypernuclei, the minimal possible number of HO quanta is $N_0 = 0$.

2.3.1   Calculation of Interaction Matrix Elements for Three-body System

For the channel subsystem (two-nucleon pair and a hyperon), the relative Jacobi coordinate described in term of scaled version of single particle coordinates is defined as
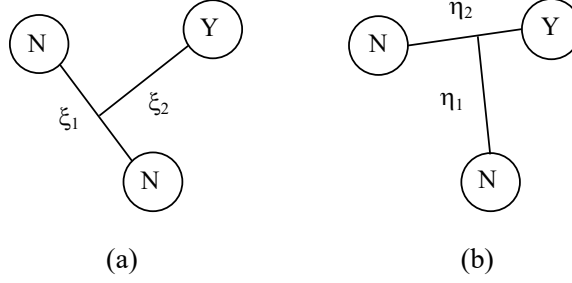
Figure 2.1 Demonstration of Jacobi coordinates employed for (a) NN pair (b) YN pair in three-body system.

$$\vec{\xi}_1 = \sqrt{\frac{1}{2}} \left(\vec{x}_1 - \vec{x}_2 \right),$$

$$\vec{\xi}_2 = \sqrt{\frac{2m_N m_Y}{2m_N + m_Y}} \left[\frac{1}{2\sqrt{m_N}} (\vec{x}_1 + \vec{x}_2) - \frac{1}{\sqrt{m_Y}} \vec{x}_3 \right],$$

(2.14)

and a JT coupled three-body HO basis depending on these coordinates $\vec{\xi}_1$ and $\vec{\xi}_2$ is constructed as

$$|(n_{NN}(l_{NN} s_{NN})j_{NN} t_{NN}, \mathcal{N}_Y \mathcal{L}_Y \mathcal{J}_Y \mathcal{T}_Y)JT\rangle,$$

(2.15)

which is appropriate for the calculation of the two-body NN interaction matrix elements $\langle V_{NN}(\vec{\xi}_1) \rangle$. The $n_{NN}, l_{NN}, s_{NN}, j_{NN}, t_{NN}$ ($\mathcal{N}_Y, \mathcal{L}_Y, \mathcal{J}_Y, \mathcal{T}_Y$) are the relative HO quantum numbers depending on the coordinate $\vec{\xi}_1$ between two nucleon (on the coordinate $\vec{\xi}_2$ between center of mass of two nucleons and a hyperon). The J and T are the total angular momentum and total isospin of the three-body system.

For a subsystem including hyperon-nucleon pair and a nucleon, the new set of Jacobi coordinate is defined as

$$\vec{\eta}_1 = \sqrt{\frac{(m_N + m_Y)m_N}{2m_N + m_Y}}$$

$$\times \left[\frac{1}{\sqrt{m_N}}\vec{x}_1 - \frac{1}{(m_N + m_Y)}(\sqrt{m_N}\vec{x}_2 + \sqrt{m_Y}\vec{x}_3) \right], \qquad (2.16)$$

$$\vec{\eta}_2 = \sqrt{\frac{m_N m_Y}{m_N + m_Y}} \left(\frac{1}{\sqrt{m_N}}\vec{x}_2 - \frac{1}{\sqrt{m_Y}}\vec{x}_3 \right),$$

where $\vec{\eta}_2$ is the relative coordinate of the YN state and $\vec{\eta}_1$ is the relative coordinate between a nucleon and the c.m. of YN pair. Consequently, using orthogonal transformation, the HO basis (2.15) can be transformed as

$$|(n_{NN}(l_{NN}s_{NN})j_{NN}t_{NN}, \mathcal{N}_Y\mathcal{L}_Y\mathcal{J}_Y\mathcal{T}_Y)JT\rangle$$

$$= \sum |(n_{NY}(l_{NY}s_{NY})j_{NY}t_{NY}, \mathcal{N}_N\mathcal{L}_N\mathcal{J}_N)JT\rangle \qquad (2.17)$$

$$\times \langle (n_{NY}(l_{NY}s_{NY})j_{NY}t_{NY}, \mathcal{N}_N\mathcal{L}_N\mathcal{J}_N)JT | (n_{NN}(l_{NN}s_{NN})j_{NN}t_{NN}, \mathcal{N}_Y\mathcal{L}_Y\mathcal{J}_Y\mathcal{T}_Y)JT\rangle.$$

The $\langle.|.\rangle$ notation is the recoupling coefficient which is given by Wigner 6-j, 9-j symbols and spacial part transformation coefficient (see detail in Appendix B). The expansion of HO basis (2.15) become

$$|(n_{NN}(l_{NN}s_{NN})j_{NN}t_{NN}, \mathcal{N}_Y\mathcal{L}_Y\mathcal{J}_Y\mathcal{T}_Y)JT\rangle = \sum_{LS} \widehat{L}^2\widehat{S}^2\widehat{j}_{NY}\widehat{\mathcal{J}}_N\widehat{j}_{NN}\widehat{\mathcal{J}}_Y$$

$$\times (-1)^{s_{NY}+1/2+s_{NN}+1/2} \begin{Bmatrix} l_{NY} & s_{NY} & j_{NY} \\ \mathcal{L}_N & 1/2 & \mathcal{J}_N \\ L & S & J \end{Bmatrix} \begin{Bmatrix} l_{NN} & s_{NN} & j_{NN} \\ \mathcal{L}_Y & 1/2 & \mathcal{J}_Y \\ L & S & J \end{Bmatrix}$$

$$\times (-1)^{t_{NY}+\mathcal{T}_N+t_{NN}+\mathcal{T}_Y}\widehat{t}_{NY}\widehat{t}_{NN} \begin{Bmatrix} 1/2 & 1/2 & t_{NN} \\ t_Y & T & t_{NY} \end{Bmatrix} (-1)^{L-\mathcal{L}_N-\mathcal{L}_Y} \qquad (2.18)$$

$$\times |(n_{NY}(l_{NY}s_{NY})j_{NY}t_{NY}, \mathcal{N}_N\mathcal{L}_N\mathcal{J}_N)JT\rangle$$

$$\times \widehat{s}_{NN}\widehat{s}_{NY} \langle \mathcal{N}_N\mathcal{L}_N n_{NY}l_{NY}|n_{NN}l_{NN}\mathcal{N}_Y\mathcal{L}_Y : L\rangle_d \begin{Bmatrix} 1/2 & 1/2 & s_{NN} \\ 1/2 & S & s_{NY} \end{Bmatrix},$$

in terms of HO basis states

$$\left| (n_{NY}(l_{NY}s_{NY})j_{NY}t_{NY}, \mathcal{N}_N\mathcal{L}_N\mathcal{J}_N)JT \right\rangle , \tag{2.19}$$

where $\left| (n_{NY}(l_{NY}s_{NY})j_{NY}t_{NY} \right\rangle$ and $\left| \mathcal{N}_N\mathcal{L}_N\mathcal{J}_N)JT \right\rangle$ are harmonic oscillator states corresponding to the hyperon-nucleon pair depending on the $\vec{\eta}_2$ coordinate and a nucleon depending on the $\vec{\eta}_1$ coordinate. The general HO bracket $\left\langle \mathcal{N}_N\mathcal{L}_N n_{NY}l_{NY} | n_{NN}l_{NN}\mathcal{N}_Y\mathcal{L}_Y : L \right\rangle_d$ mediates the spacial part transformation between two coordinate sets $\vec{\xi}_1, \vec{\xi}_2$ and $\vec{\eta}_2, \vec{\eta}_1$ which couple to the total angular momentum L. The coordinate transformation can be put into the form of Ref. (Kamuntavicius et al., 2001)

$$\begin{pmatrix} \vec{\eta}_2 \\ \vec{\eta}_1 \end{pmatrix} = \begin{pmatrix} \sqrt{\dfrac{d}{1+d}} & \sqrt{\dfrac{1}{1+d}} \\ \sqrt{\dfrac{1}{1+d}} & \sqrt{\dfrac{1}{1+d}} \end{pmatrix} \begin{pmatrix} \vec{\xi}_1 \\ \vec{\xi}_2 \end{pmatrix} , \tag{2.20}$$

with the mass radio $d = \frac{m_Y}{2m_N+m_Y}$. The two-body YN interaction matrix elements are calculated in the basis (2.19) through the basis expansion (2.18)

$$\left\langle \sum_{i=1}^{2} V_{YN}(\vec{r}_i, \vec{r}_3) \right\rangle = 2 \left\langle V_{YN}(\vec{\eta}_2) \right\rangle . \tag{2.21}$$

The matrix element $\left\langle V_{YN}(\vec{\eta}_2) \right\rangle$ is diagonal in all quantum numbers of the states (2.19), excluding n_{NY} and l_{NY}. The computational model space is characterized by the maximum number of HO quanta in the basis states (2.15) as

$$2n_{NN} + l_{NN} + 2\mathcal{N}_Y + \mathcal{L}_Y \leq N_{\max}, \tag{2.22}$$

where $N_{\max}$ is the maximum number of oscillator quanta shared by all three particles above the lowest HO configuration. The total energies of three-body systems $^3_\Lambda H$ and Λnn are calculated by diagonalization of Hamiltonian (2.2) between the basis states in Eq. (2.15). The corresponding results are presented in the next chapter.

2.3.2 Calculation of Interaction Matrix Elements for Four-body System

Analogs to the construction of three-body HO basis, the first set of Jacobi-coordinates for a four-body hypernuclear system (three-nucleon pair and a hyperon) is defined as

$$\vec{\xi}_1 = \sqrt{\frac{1}{2}}(\vec{x}_1 - \vec{x}_2),$$

$$\vec{\xi}_2 = \sqrt{\frac{2}{3}}\Big[\frac{1}{2}(\vec{x}_1 + \vec{x}_2) - \vec{x}_3)\Big], \qquad (2.23)$$

$$\vec{\xi}_3 = \sqrt{\frac{3mm_Y}{3m + m_Y}}\Big[\frac{1}{2\sqrt{m}}(\vec{x}_1 + \vec{x}_2 + \vec{x}_3) - \frac{1}{\sqrt{m_Y}}\vec{x}_4\Big],$$

where $\vec{\xi}_1$ is the relative coordinate of two nucleon pair, $\vec{\xi}_2$ is the relative coordinate between c.m. of two nucleon pair and a third nucleon, $\vec{\xi}_3$ is the relative coordinate between a hyperon and the c.m. of the three nucleons. The antisymmetrized four-body HO basis (A.7) depending on the coordinates $\vec{\xi}_1$, $\vec{\xi}_2$ and $\vec{\xi}_3$ is expressed as

$$\big|(N_{NNN}i_{NNN}J_{NNN}T_{NNN}, \mathcal{N}_Y\mathcal{L}_Y\mathcal{J}_Y\mathcal{T}_Y)JT\big\rangle, \qquad (2.24)$$

which is suitable for the calculation of the three-body NNN interaction matrix elements. The quantum number i_{NNN} distinguishes between different antisymmetric states with the same quantum numbers $N_{NNN}, J_{NNN}, T_{NNN}$. A NNN basis depending on Jacobi coordinates $\vec{\xi}_1$ and $\vec{\xi}_2$ is

$$\big|N_{NNN}i_{NNN}J_{NNN}T_{NNN}\big\rangle = \sum \mathrm{cfp}$$
$$\times \big|n_{NN}(l_{NN}s_{NN})j_{NN}t_{NN}, \mathcal{N}_N\mathcal{L}_N\mathcal{J}_N, J_{NNN}T_{NNN}\big\rangle, \qquad (2.25)$$

where cfp is the coefficients of fractional parentage obtained from three-body NNN basis antisymmetrization (see detail in Appendix A). $\big|(n_{NN}(l_{NN}s_{NN})j_{NN}t_{NN}\big\rangle$ and $\big|\mathcal{N}_N\mathcal{L}_N\mathcal{J}_N\big\rangle$ are harmonic oscillator states related to the NN pair depending on the coordinate $\vec{\xi}_1$ and a third nucleon depending

on the coordinate $\vec{\xi}_2$. The three-body NNN interaction matrix elements are calculated in the basis (2.24) as

$$\langle V_{NNN}(\vec{r}_1, \vec{r}_2, \vec{r}_3) \rangle = \langle V_{NNN}(\vec{\xi}_1, \vec{\xi}_2) \rangle. \tag{2.26}$$

The matrix elements $\langle V_{NNN}(\vec{\xi}_1, \vec{\xi}_2) \rangle$ are diagonal in all quantum numbers of the state (2.24) expect for N_{NNN} and i_{NNN}, for isospin-invariant interactions.
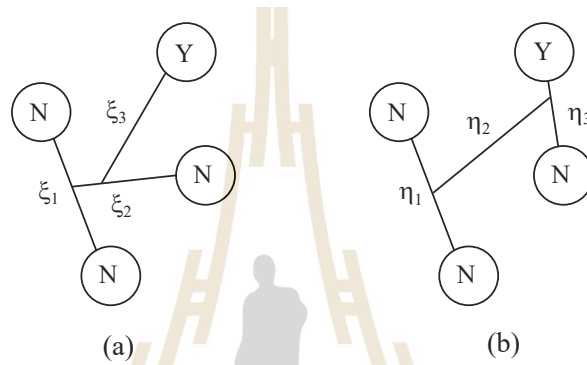
Figure 2.2 Demonstration of Jacobi coordinates employed for (a) antisymmetrization and NNN interaction (b) NN and YN interactions.

The constructed antisymmetrized basis (2.24) is not appropriate for the calculation of two-body interaction matrix elements. The new set of Jacobi coordinates is required when the NN and YN interaction matrix elements need to be calculated. The new set is acquired from the first set (2.23) by keeping the c.m. coordinate $\vec{\xi}_0$, $\vec{\xi}_1$ and introducing two different variables as follows

$$\vec{\xi}_0, \vec{\xi}_1 = \vec{\eta}_1,$$

$$\vec{\eta}_2 = \sqrt{\frac{2m_N(m_N + m_Y)}{3m_N + m_Y}}$$

$$\times \left[\frac{1}{\sqrt{2m_N}}(\vec{x}_1 + \vec{x}_2) - \frac{1}{m_N + m_Y}(\sqrt{m_N}\vec{x}_3 + \sqrt{m_Y}\vec{x}_4) \right], \tag{2.27}$$

$$\vec{\eta}_3 = \sqrt{\frac{(m_N m_Y)}{m_N + m_Y}} \left(\frac{1}{m_N}\vec{x}_3 - \frac{1}{\sqrt{m_Y}}\vec{x}_4 \right),$$

where $\vec{\eta}_1$ is the relative coordinate of two nucleon pair, $\vec{\eta}_2$ is the relative coordinate between c.m. of the hyperon-nucleon pair and c.m. of the two nucleon pair. $\vec{\eta}_3$ is the relative coordinate of the YN pair. Using orthogonal transformation, the basis (2.24) is transformed to a basis containing antisymmetrized nucleon-nucleon state and hyperon-nucleon state

$$|(N_{NNN}i_{NNN}J_{NNN}T_{NNN}, \mathcal{N}_Y\mathcal{L}_Y\mathcal{J}_Y\mathcal{T}_Y)JT\rangle$$

$$= \sum \mathrm{cfp}(-1)^{t_{NN}+1/2+\mathcal{T}_Y+T+J_{NN}+j_N+J_{NNN}+J+\mathcal{L}'+j_{NY}+I_N+\mathcal{L}_Y+s_{NY}}$$

$$\times \hat{T}_{NNN}\hat{t}_{NY}\hat{\mathcal{J}}_Y\hat{J}_{NNN}\hat{I}^2_{NY}\hat{j}_N\hat{s}_{NY}\hat{I}_{NY}\hat{j}_{NY} \begin{Bmatrix} I_N & 1/2 & j_N \\ \mathcal{L}_Y & 1/2 & \mathcal{J}_N \\ I_{NY} & s_{NY} & \mathcal{J} \end{Bmatrix}$$ (2.28)

$$\times \begin{Bmatrix} \mathcal{L}_Y & \mathcal{J} & I_{NY} \\ s_{NY} & l_{NY} & j_{NY} \end{Bmatrix} \begin{Bmatrix} T_{NN} & 1/2 & T_{NNN} \\ \mathcal{T}_Y & T & t_{NY} \end{Bmatrix} \begin{Bmatrix} j_{NN} & j_N & J_{NNN} \\ \mathcal{J}_Y & J & \mathcal{J} \end{Bmatrix}$$

$$\times \langle n_{NY}l_{NY}\mathcal{N}'\mathcal{L}'I_{NY}|\mathcal{N}_Y\mathcal{L}_Y n_N I_N I_{NY}\rangle_d$$

$$\times |n_{NN}l_{NN}s_{NN}j_{NN}t_{NN}, (n_{NY}l_{NY}s_{NY}j_{NY}t_{NY}, \mathcal{N}'\mathcal{L}')\mathcal{J}, JT\rangle,$$

in term of HO basis states

$$|n_{NN}l_{NN}s_{NN}j_{NN}t_{NN}, (n_{NY}l_{NY}s_{NY}j_{NY}t_{NY}, \mathcal{N}\mathcal{L})\mathcal{J}, JT\rangle, \quad (2.29)$$

where $|n_{NN}l_{NN}s_{NN}j_{NN}t_{NN}\rangle$ and $|n_{NY}l_{NY}s_{NY}j_{NY}t_{NY}\rangle$ correspond to nucleon-nucleon state depending on the $\vec{\eta}_1$ coordinate and hyperon-nucleon state depending on the coordinate $\vec{\eta}_3$. The state $|\mathcal{N}\mathcal{L}\rangle$ depends on the $\vec{\eta}_2$ coordinate. The calculation of the general HO bracket $\langle n_{NY}l_{NY}\mathcal{N}'_Y\mathcal{L}'_Y I_{NY}|\mathcal{N}\mathcal{L}n_N I_N I_{NY}\rangle_d$ needs two coordinate sets $\vec{\xi}_2, \vec{\xi}_3$ and $\vec{\eta}_3, \vec{\eta}_2$ which are connected by the orthogonal transformation (Kamuntavicius et al., 2001),

$$\begin{pmatrix} \vec{\eta}_3 \\ \vec{\eta}_2 \end{pmatrix} = \begin{pmatrix} \sqrt{\dfrac{d}{1+d}} & \sqrt{\dfrac{1}{1+d}} \\ \sqrt{\dfrac{1}{1+d}} & \sqrt{\dfrac{1}{1+d}} \end{pmatrix} \begin{pmatrix} \vec{\xi}_2 \\ \vec{\xi}_3 \end{pmatrix}, \quad (2.30)$$

where $d = \frac{2*m_Y}{3m+m_Y}$ is the mass radio of the involved particles. With the help of basis expansion (2.28), the two-body YN and NN interaction matrix elements can be calculated in the basis (2.29) as

$$\langle \sum_{i<j=1}^{3} V_{NN}(\vec{r_i}, \vec{r_j}) \rangle = 3 \langle V_{NN}(\vec{\eta_1}) \rangle, \tag{2.31}$$

and

$$\langle \sum_{i=1}^{3} V_{YN}(\vec{r_i}, \vec{r_4}) \rangle = 3 \langle V_{YN}(\vec{\eta_3}) \rangle, \tag{2.32}$$

where the $\langle V_{NN}(\vec{\eta_1}) \rangle$ and $\langle V_{YN}(\vec{\eta_3}) \rangle$ matrix elements are diagonal in all quantum numbers of the state (2.29) expect for the quantum numbers n and l. The computational model space is restricted by maximal four-body HO basis truncation as

$$2n_{NN} + l_{NN} + 2\mathcal{N}_N + \mathcal{L}_N + 2\mathcal{N}_Y + \mathcal{L}_Y \leq N_{\max}, \tag{2.33}$$

where $N_{\max}$ is the maximum number of oscillator quanta shared by all four particles above the lowest HO configuration. The total energies of four-body systems $^4_\Lambda H$ and $^4_\Lambda He$ are calculated by diagonalization of Hamiltonian (2.2) between the basis states, which are presented in chapter III.

2.4   IR Extrapolation

IR extrapolation can be utilized to estimate the infinite results from smaller model spaces (Furnstahl et al., 2012; Coon et al., 2012; Wendt et al., 2015). The computational finite HO basis defined by the model space ($N_{\max}$) and HO frequency ($\hbar\omega$) can be described by the corresponding infrared (IR) length and ultraviolet (UV) scales.

In the NCSM basis specified by a total energy truncation, the IR length scale (L_{eff}) can be computed by evaluating the discrete kinetic energy spectrum in hyperradial well and NCSM space (Wendt et al., 2015). A brief description of the calculation of infrared (IR) length scales is presented in Appendix D. The leading

order IR extrapolation formula (Furnstahl et al., 2012) for energies is

$$E(L_{eff}) = E_\infty + a_0 e^{(-2k_\infty L_{eff})}, \qquad (2.34)$$

where E_∞, a_0 and k_∞ are the fit parameters. When the IR extrapolation is invalid at where the final energy is above the variational minimum energy calculated in a NCSM space with $N_{\max}^{tot}$, IR corrections need to be considered in the extrapolation. Subleading IR corrections to a leading order IR extrapolation formula, have the suggested form (Forssén et al., 2018)

$$\sigma_{IR} \propto \frac{e^{-2k_\infty L_{eff}}}{k_\infty L_{eff}}. \qquad (2.35)$$

The inclusion of subleading IR correction in the extrapolation will push the extrapolated parameter E_∞ down under the variational minimum E_{varmin}.

The extrapolated results will depend on the selected UV scales. To achieve UV-convergence, UV cutoff Λ_{UV} needs to be higher than chiral regulator cutoff Λ_{NN} used in chiral effective field theory. We use a fixed UV cutoff $\Lambda_{\mathrm{UV}} = 1200$ MeV (Forssén et al., 2018) because a higher UV cutoff is needed in many-body basis to capture all UV physics included in NN interactions. Then UV corrections to finite-space results can be important unless $\Lambda_{\mathrm{UV}} \gg \Lambda_{NN}, \Lambda_{YN}$. Here there is no need for UV correction because a fixed UV cutoff $\Lambda_{\mathrm{UV}} = 1200$ MeV is sufficient for this calculation. Only the UV converged energy points are selected for extrapolation. The IR extrapolation formula (2.34) is still valid at a selected UV cutoff $\Lambda_{\mathrm{UV}} = 1200$ MeV (Forssén et al., 2018). The UV converged data can be obtained by doing calculations at corresponding $(N_{\max}, \hbar\omega)$ model-space parameters.

CHAPTER III

CONVERGENCE PROPERTIES AND UNCERTAINTY

QUANTIFICATION OF HYPERNUCLEI

In this chapter, we study the convergence properties and the dependence of hypernuclear binding energy on various model space sizes and HO frequencies. We then analyze the sensitivity of the s-shell hypernuclear binding energies to systematic nuclear uncertainties.

3.1   Systematic Uncertainties of Nuclear Interactions

The chiral NN interaction model depends on the choice of regular cutoffs Λ in the chiral NN potentials, selection of the experimental data for fitting and the truncation of the chiral expansion. The family of 42 different nuclear interactions at NNLO (labeled NNLO$_{sim}$) (Carlsson et al., 2016) was constructed by varying the chiral momentum cutoff parameter Λ_{NN} between 450 and 600 MeV in steps of 25 MeV and the truncation of the input NN scattering $T_{max} \leq T_{Lab}^{max}$ between 125 and 290 MeV in six steps. All nuclear potential models indicate an equally good description of the NN scattering. These model errors are also called systematic model uncertainties. For each 42 different potential models, all 26 low-energy constants (LECs) up to NNLO were optimised to NN and πN scattering and few-body nuclear bound-state observables at the same time: $^{2,3}H$, ^{3}He. Each LECs also have small statistical uncertainties from the fit. But it does not have much effect on a predicted observable if we compare with systematic uncertainties. So, we focus our attention on the study of the systematic nuclear uncertainty effect on predicted hyernuclear binding energy.

3.2   Binding Energies of Hypernuclear Systems

We here present the ground state and excited state binding energies of three- and four-body hypernuclear systems and discuss the consequence of our findings.

3.2.1 Three-Body Λnn System and $^{3}_{\Lambda}H$ Hypernucleus

The three-body systems are analyzed within the NCSM framework using chiral NNLO NN interaction with momentum cutoff $\Lambda_{NN} = 500$ MeV and LO YN interaction with $\Lambda_{YN} = 600$ MeV. We have computed the total energy of Λnn system in the oscillator basis with model space up to $N_{\max} = 36$ MeV in the range of the HO frequencies 1 MeV $\leq \hbar\omega \leq 40$ MeV. It is found that there is no Λnn bound system. The ground-state Λnn energies as a function of HO frequencies $\hbar\omega$ and model space sizes $N_{\max}$ are presented in Figure 3.1. The solid black lines represent the predicted binding energies obtained from interpolation between each data point. The NCSM energies decrease with increasing of $N_{\max}$ and with decreasing of $\hbar\omega$. Then we continue the study of the Λnn resonance within SS-HORSE extension of the NCSM to the continuum. The calculation of 3 $\rightarrow$ 3 scattering phase shifts will be presented in chapter IV.
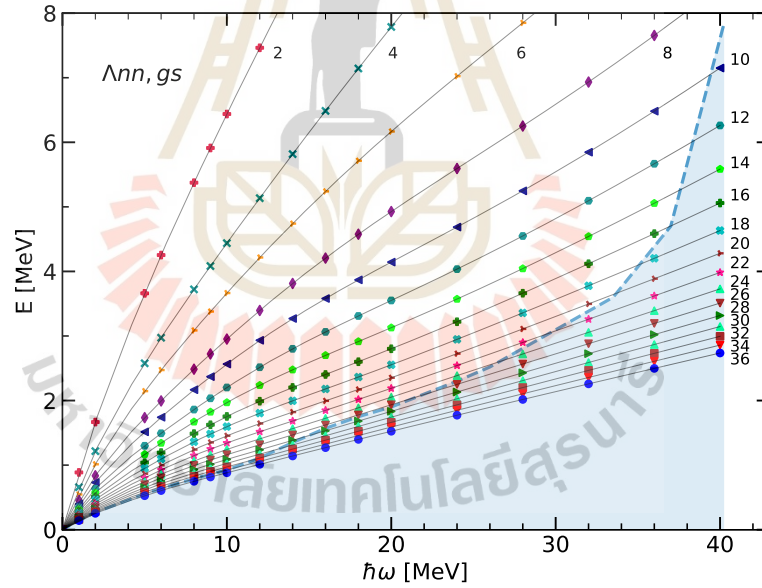
Figure 3.1 The Λnn eigenenergy $E(\Lambda nn)$ dependence on the HO frequency $\hbar\omega$, computed using the NNLO$_{\text{sim}}$ interaction $\Lambda_{NN} = 500$ MeV and $T^{\max}_{\text{Lab}} = 290$ MeV for different model-space sizes from $N_{\max} = 2$ to $N_{\max} = 36$. Blue shaded area shows the selected energies for parametrization of the scattering amplitude.

For the $^{3}_{\Lambda}H$ system, the calculations of total energy are performed in the model space $N_{\max}$ up to 66 MeV and in the range of the HO frequencies $7 \leq \hbar\omega \leq 40$ MeV by using a chiral LO YN interaction and chiral NNLO$_{\text{sim}}$NN
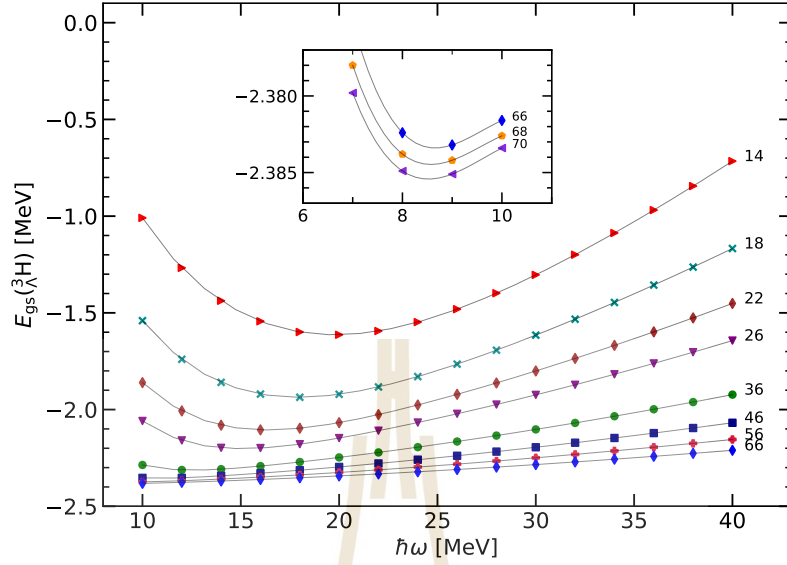
Figure 3.2 The hypertriton ground state energy $E({}^3_\Lambda H)$ dependence on the HO frequency $\hbar\omega$, computed using the NNLO$_{\text{sim}}$ interaction $\Lambda_{NN} = 500$ MeV and $T^{\text{max}}_{\text{Lab}} = 290$ MeV for different model-space sizes from $N_{\text{max}} = 14$ to $N_{\text{max}} = 70$.

interactions. We choose one of the 42 nuclear interactions ($\Lambda_{NN} = 500$ MeV, $T^{\text{max}}_{\text{Lab}} = 290$ MeV), which is the standard choice in nuclear calculations, to study more detail about the convergence behaviors. The ground-state energy of hypertriton for different model space sizes and HO frequencies is presented in Figure 3.2, for a particular interaction ($\Lambda_{NN} = 500$ MeV, $T^{\text{max}}_{\text{Lab}} = 290$ MeV). The hypertriton energy is converging with the increasing of the model space size while the dependence on $\hbar\omega$ decreases. But the convergence is very slow due to the very weak hypertriton binding energy. We also searched for the eigenenergy values at $\hbar\omega = 7, 8, 9$ MeV with the largest model space sizes to locate the variational minimum. The optimal energy $E_{\text{varmin}}({}^3_\Lambda H) = -2.385$ MeV for this particular interaction is occurred at the HO frequency $\hbar\omega = 9$ MeV and $N_{\text{max}} = 70$ MeV. Calculations of ${}^3_\Lambda H$ in the model spaces up to $N_{\text{max}} = 70$ MeV show that the resulting variational minimum energy is converged enough.

We furthermore study the convergence of variational minimum by applying IR extrapolation technique to our NCSM results computed in model space specified
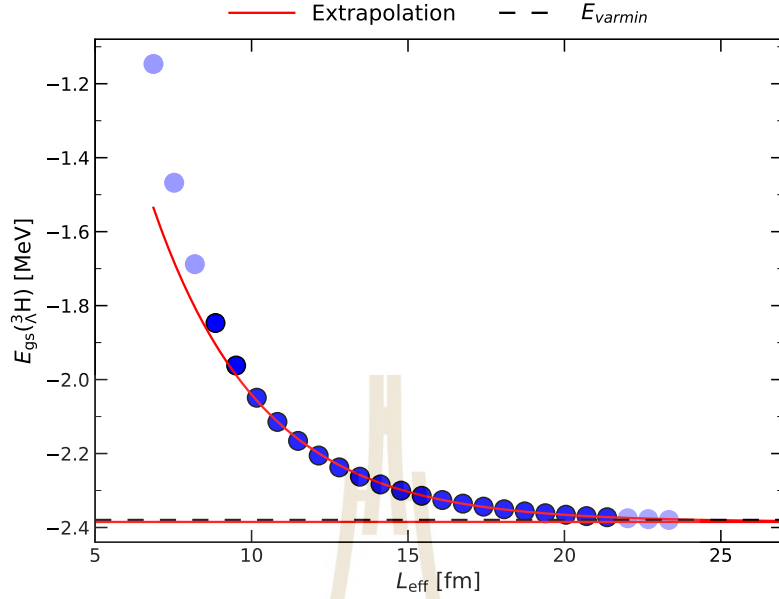
Figure 3.3 Extrapolation of $E\left(^{3}_{\Lambda}H\right)$ computed using the NNLO$_{\text{sim}}$ interaction $\Lambda_{NN} = 500$ MeV and $T^{\max}_{\text{Lab}} = 290$ MeV for a fixed $\Lambda_{\text{UV}} = 1200$ MeV. The data $N_{\max} \in [22, 60]$ points are used in the fit.

by corresponding IR length scale L_{eff} at $\Lambda_{\text{UV}} = 1200$ MeV. We perform fits to Eq. (2.34) with an NLO correction term in Eq. (2.35) to get more stabilized results. All UV converged energy points included in our exponential fitting are described by dark blue makers. The extrapolated energy $E_{\infty}(^{3}_{\Lambda}H) = -2.385$ MeV obtained from fitting with data $N_{\max} \in [22, 60]$ is shown by a red horizontal line in Figure 3.3. The energy difference between E_{varmin} at $N_{\max} = 66$ and E_{∞} for this nuclear interaction ($\Lambda_{NN} = 500$ MeV and $T^{\max}_{\text{Lab}} = 290$ MeV) is just a few keV. It indicates that uncertainty of many-body method is negligible.

The experimental binding energy for hypertriton is $E^{exp.}\left(^{3}_{\Lambda}H\right) = -2.35 \pm 0.05$ MeV (Davis, 2005). For other 41 nuclear Hamiltonians, we assume that the final conclusion for convergence study will be the same. The predicted results of hypertriton system have been published (Htun et al., 2021).

3.2.2 Four-Body $^{4}_{\Lambda}H$ and $^{4}_{\Lambda}He$ Hypernuclei

NCSM calculations are performed for the four-body hypernuclear systems using chiral nuclear interactions (NN+NNN) at approximate ($N_{\max}, \hbar\omega$) model-space
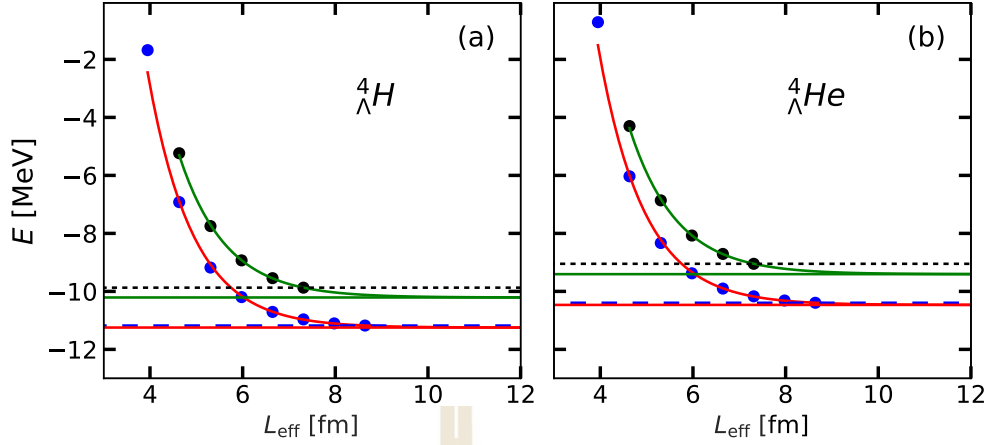
Figure 3.4 (a-b) Extrapolations of the total energy for both ground state and excited state of $^{4}_{\Lambda}H$ and $^{4}_{\Lambda}He$ for $\Lambda_{NN} = 500$ MeV and $T^{\mathrm{max}}_{\mathrm{Lab}} = 290$ MeV NN interaction. The solid red (green) line and the dash blue (black) line indicate the extrapolated and variational minimum energies in the largest model space $N_{\mathrm{max}} = 20$ (16) MeV for $0^{+}(1^{+})$ states, respectively.

parameters associated with a high UV cutoff $\Lambda_{\mathrm{UV}} = 1200$ MeV. The computed IR length scales L_{eff} and the HO frequencies $\hbar\omega$ for all corresponding systems are tabulated in Table D.1. The ground and excited states binding energies of both $^{4}_{\Lambda}H$ and $^{4}_{\Lambda}He$ hypernuclei are obtained with model spaces $N_{\mathrm{max}} \leq 20$ MeV and $N_{\mathrm{max}} \leq 16$ MeV, respectively. The model space is enough to get converged values in $^{4}_{\Lambda}H$ and $^{4}_{\Lambda}He$ with the bare LO YN and NNLO$_{\mathrm{sim}}$ NN interactions. The NCSM computation going to larger N_{max} is difficult and costly when involved particles increase. We show the model-space dimensions of our calculated hypernuclei with different N_{max} in Figure C.1.

The IR extrapolation is applied to extract the final binding energy from smaller model spaces. The only UV converged energy points obtained with $\Lambda_{\mathrm{UV}} = 1200$ MeV are included in our simple fitting to Eq. (2.34). The fits are performed with the data $N_{\mathrm{max}} \in [6, 20]$ for ground state and with the data $N_{\mathrm{max}} \in [8, 16]$ for excited state. Figure 3.4 shows the extrapolations with NLO correction term for the ground state and excited state of $^{4}_{\Lambda}H$ and $^{4}_{\Lambda}He$. We can see that the convergence with the size of the model space is much faster for more bound hypernuclear systems. But every heavier hypernuclear system are not always

feasible to reach convergence. Then we compute the ground state Λ-separation energies, $E_\Lambda = E(^{A-1}Z) - E(^A_\Lambda Z)$, of all relevant hypernuclei and compare with their experimental Λ binding energy which is presented in Table 3.1. We found that the Λ-separation energy of $^4_\Lambda H$ hypernucleus is overbinding than the experimental one for this particular NN interactions.

Table 3.1 The Λ-separation energies obtained with $NNLO_{sim}(\Lambda_{NN} = 500$ MeV, $T^{max}_{Lab} = 290$ MeV) for bound-state light hypernuclei.

Hypernuclei	Experimental value (MeV)	Reference	$E_{gs,\infty}$ (MeV)	$E^{sep}_{\Lambda,\infty}$ (MeV)
$^3_\Lambda H$	0.13 ± 0.05	[(Davis, 2005)]	-2.385	0.161
$^4_\Lambda H$	2.04 ± 0.04	[(Davis, 2005)]	-11.248	2.766
$^4_\Lambda He$	2.39 ± 0.03	[(Davis, 2005)]	-10.467	2.750

3.3 Systematic Uncertainties of $^3_\Lambda H$, $^4_\Lambda H$ and $^4_\Lambda He$ Hypernuclei

Since we have presented that we can reach converged results, the calculations with all 42 interaction models are performed to quantify the magnitude of model variations in $^3_\Lambda H$, $^4_\Lambda H$ and $^4_\Lambda He$ hypernuclei. The resulting spread in the hypertriton binding energies from 42 independent calculations using $N_{max} = 66$ and $\hbar\omega = 9$ MeV are shown in Figure 3.5. The NCSM eigenenergies decrease with increasing momentum cutoff and increase with increasing T^{max}_{Lab}. The obtained spread in binding energy predictions express the model uncertainties of $E(^3_\Lambda H)$ due to the quantified uncertainty of nuclear structure models. We find that the systematic nuclear uncertainty in $E(^3_\Lambda H)$ is rather small. It is about $\lesssim 100$ keV and almost the same as the experimental uncertainties of hyertriton.

The E_∞ values obtained in this way for all 42 different NN nuclear interactions follow the same trend in $^4_\Lambda H$ and $^4_\Lambda He$ (see Figure 3.7). The variational results are obtained with $N_{max} = 20$ and $\hbar\omega = 29.19$ MeV for ground states and $N_{max} = 16$ and $\hbar\omega = 34.49$ MeV for excited states of four-body hypernuclei. The extrapolation are performed at $\Lambda_{UV} = 1200$ MeV including NLO correction

terms. The uncertainties of variational minimum energies, E_{varmin} and extrapolated energies, E_∞ are summarized in Table 3.2. The magnitudes of the spread of four-body hypernuclear binding energies indicate that our results are not extremely sensitive to the uncertainty of NN interactions. The entire model uncertainties of extrapolated Λ-separation energies obtained from 42 NNLO$_{\text{sim}}$ NN interactions for $^{4}_{\Lambda}H$ are overbind than the experimental uncertainties. Although the calculations with YN and NN-forces only for the four-body systems give much larger uncertainty, the inclusion of the three-body nucleon forces provides the smaller dependence of total binding energy on the uncertainties of nuclear interaction. This finding of the modest systematic uncertainties opens up the opportunity to utilize the binding energies of $^{3}_{\Lambda}H$ and $^{4}_{\Lambda}He$ hypernuclei as the relevant bound state observables to constrain YN interaction models.

Table 3.2 Uncertainty ranges of the variational minimum energies and extrapolated energies for ground and excited states of four-body hypernuclei.

Hypernuclei	E_{varmin}(MeV)		E^{NLO}_∞(MeV)	
	Range	$\sigma^{\text{var.}}_{\text{model}}$	Range	$\sigma^\infty_{\text{model}}$
$^{4}_{\Lambda}H(0^+)$	-11.272 ... -10.749	0.523	-11.337 ... -10.856	0.481
$^{4}_{\Lambda}H(1^+)$	-9.941 ... -9.471	0.328	-10.269 ... -9.890	0.419
$^{4}_{\Lambda}He(0^+)$	-10.484 ... -9.970	0.514	-10.554 ... -10.082	0.472
$^{4}_{\Lambda}He(1^+)$	-9.117 ... -8.655	0.462	-9.463 ... -9.094	0.369
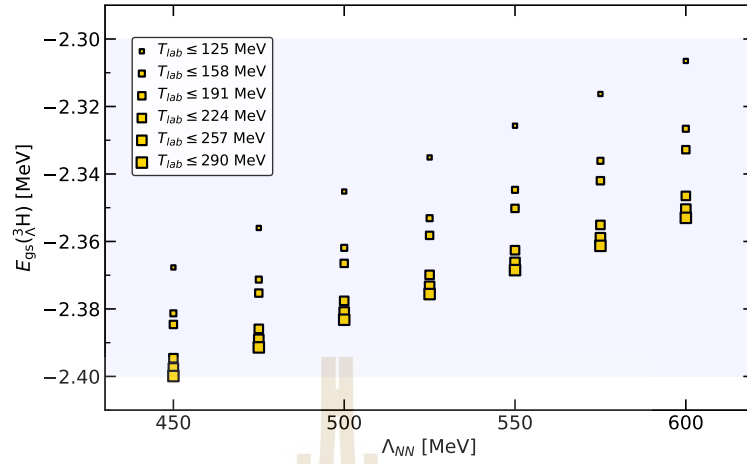
Figure 3.5 Binding energy predictions for $^{3}_{\Lambda}H$ (variational minima at $N_{\max} = 66$ and $\hbar\omega = 9$ MeV) with the 42 different NNLO$_{\text{sim}}$ interaction models. The blue band represents the experimental binding energies $E_{\exp.}(^{3}_{\Lambda}H) = $ -2.35 $\pm$ 0.05 MeV.
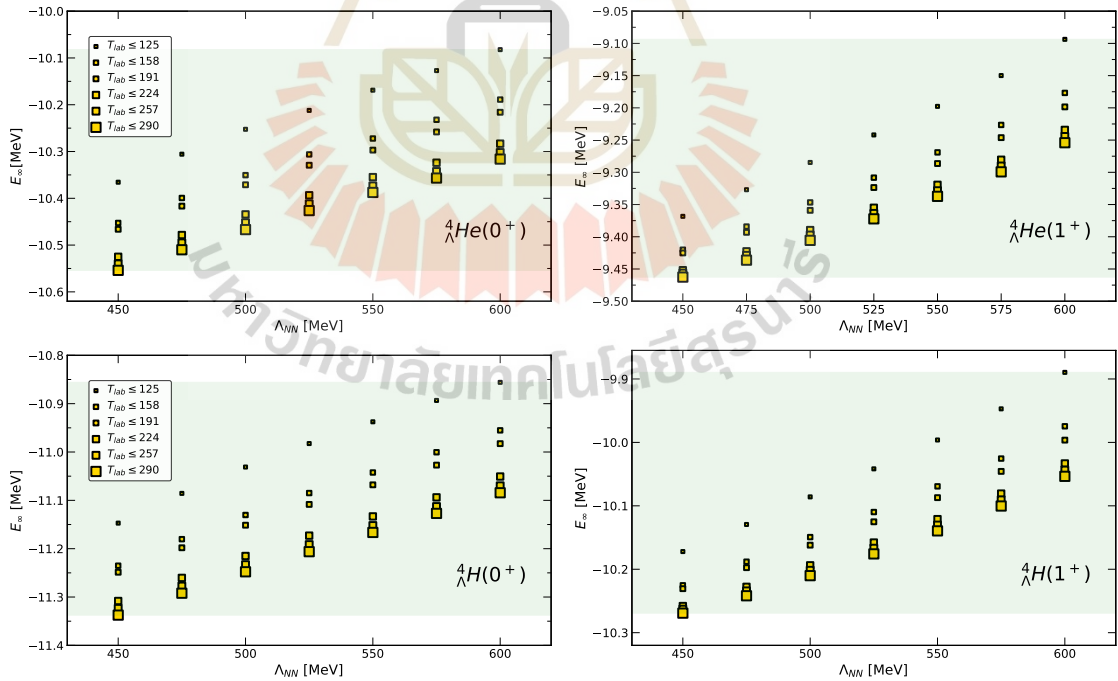
Figure 3.6 Ground state energies for $^{4}_{\Lambda}H$ and $^{4}_{\Lambda}He$ with the 42 different NNLO$_{\text{sim}}$ interaction models. The green band represents the model uncertainty in hypernuclei.
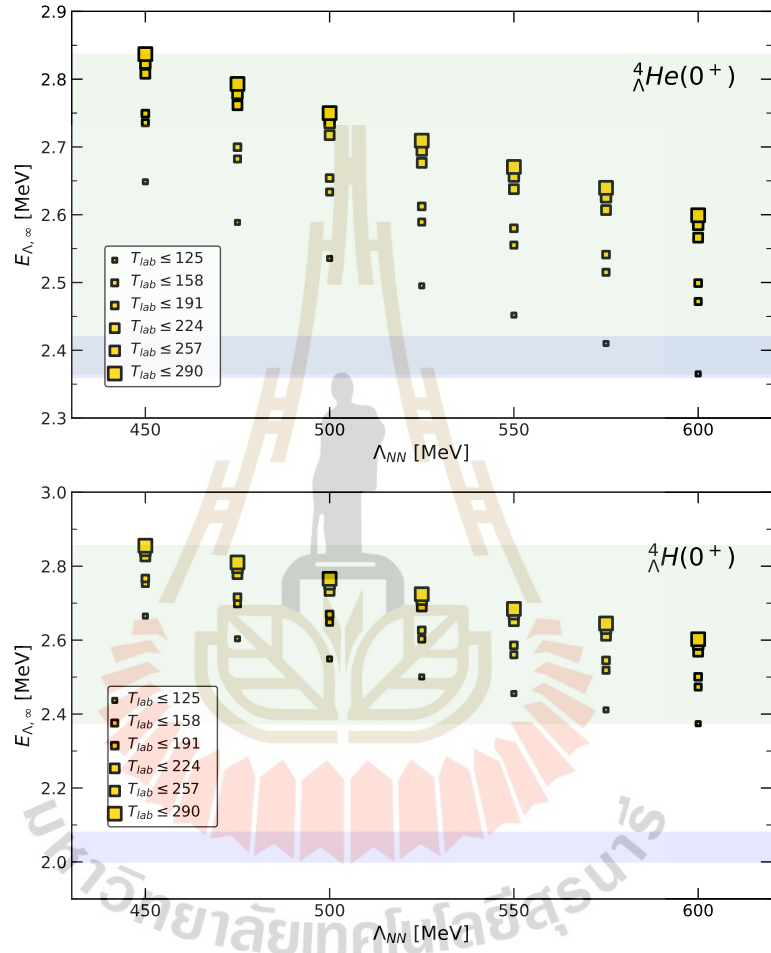
Figure 3.7 Ground state Λ-separation energies for $^4_\Lambda H$ and $^4_\Lambda He$ with the 42 different NNLO$_{sim}$ interaction models. The green band represents the model uncertainty in hypernuclei. The experimental Λ-binding energies are $^4_\Lambda H \sim 2.04 \pm 0.04$ MeV and $^4_\Lambda He \sim 2.39 \pm 0.03$ MeV, presented by a blue band.

CHAPTER IV

CALCULATION OF LOW ENERGY PHASE SHIFTS AND

RESONANT PARAMETERS

Assuming that the NCSM final energy of Λnn is an estimation to the resonance energy, we extend NCSM to the continuum state by employing J-Matrix formalism (Bang et al., 2000; Yamany and Fishman, 1975), also known as Harmonic oscillator representation of scattering equation (HORSE) formalism, which allows us to study continuum spectrum using only positive energies obtained from bound state approaches like NCSM applying harmonic oscillator basis. The HORSE method can be used to describe the open channels in the external subspace while the internal subspace is associated with NCSM approach.

4.1   Hyperspherical Coordinate for Λnn System

The similar three-body Jacobi coordinate set described in Chp. II. is used for Λnn system as

$$
\begin{aligned}
\vec{\xi}_1 &= \sqrt{\frac{1}{2}}\left(\vec{x}_1 - \vec{x}_2\right), \\
\vec{\xi}_2 &= \sqrt{\frac{2m_n m_Y}{2m_n + m_Y}}\left[\frac{1}{2\sqrt{m_n}}(\vec{x}_1 + \vec{x}_2) - \frac{1}{\sqrt{m_Y}}\vec{x}_3\right],
\end{aligned}
\tag{4.1}
$$

where $\vec{\xi}_1$ $(\vec{\xi}_2)$ is correspond to the relative coordinate of the two neutron (between the c.m. coordinate of the two neutron pair and a hyperon).

For a given choice of three-body Jacobi vector $(\vec{\xi}_1, \vec{\xi}_2)$, the configuration of the system is expressed by the six parameters, $\xi_1, \xi_2, \theta_1, \theta_2, \phi_1, \phi_2$, including the polar angles $\widehat{\xi}_i \equiv (\theta_i, \phi_i)$ of each Jacobi vector. The two radii ξ_1, ξ_2 have infinite ranges and the others vary within finite limits. The first two variables can be changed to the hyperradius ρ and hyperangle β which are defined respectively as

$$\rho = \sqrt{\xi_1^2 + \xi_2^2}, \tag{4.2}$$

and

$$\beta = \tan^{-1}\frac{\xi_2}{\xi_1}, \tag{4.3}$$

to run one variable ρ from zero to infinite while the other five variables vary within finite limits, where $\xi_1 = \rho\cos(\beta)$ and $\xi_2 = \rho\sin(\beta)$. The hyper radius ρ is the collective size of the system. The six parameters now become

$$\rho, \beta, \theta_1, \theta_2, \phi_1, \phi_2. \tag{4.4}$$

In the following, we use the notation $\Omega_5 \equiv (\beta, \theta_1, \theta_2, \phi_1, \phi_2)$ for hyperspherical polar angles. In hyperspherical formalism, three-body system is described in six-dimensional hyperspherical space having hyper radius and five hyperspherical angles. Generally speaking, the hyperspherical coordinate is a magic coordinate having hyper radius which measures the distance between all three particles at once which also have some relative angular momentum.

The hyperradial part of free Schrodinger equation for three-body system is

$$\left(-\frac{\partial^2}{\partial\rho^2} + \frac{\mathcal{L}(\mathcal{L}+1)}{\rho^2} - q^2 \right) u_K(E, \rho) = 0, \tag{4.5}$$

where the effective angular momentum $\mathcal{L} = K + \dfrac{3A-6}{2}$ and $q = \sqrt{\dfrac{2E}{\hbar\omega}}$ is dimensionless momentum. The hypermomentum K, also called grand angular momentum, can be obtained by the sum of intrinsic orbital angular momenta. Note that K in Λnn calculation is the angular momentum in six-dimensional space.

4.2   Democratic Decay Approximation

In the extension into continuum, the three-body extension of the J-matrix formalism for all three-body Λnn decay channels is very complicated. We utilize the democratic decay approximation (also known as true three-body scattering or

3 → 3 scattering) (Zaitsev et al., 1998) to describe the Λnn system decaying through only three-body break-up channel. The other possible two-body channels associated with two-body sub-bound systems nn and Λn are not allowed in this approximation. A decay of a system into A particles is called 'democratic' if no sub-bound systems is in the decaying process. In the asymptotic limit, all three particles are well separated from each other and they fly away freely. Democratic decay approximation employs a complete hyperspherical harmonics (HH) basis to describe the continuum spectrum. The illustration for democratic 3 → 3 scattering is shown in Figure 4.1.
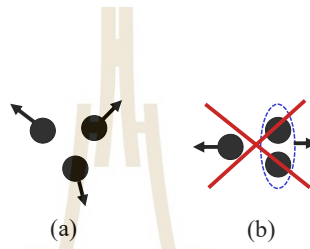
Figure 4.1 Illustration for three-body democratic decaying (a) and no sub-bound system (b).

4.3 J-Matrix Formalism with Hyperspherical Oscillator Basis

The J-Matrix approach (Yamany and Fishman, 1975), also known as HORSE method, can be used to extend the finite NCSM Hamiltonian matrix in the HO basis into the continuum. The total wave function of the system is generally described as a function of the (A - 1) jacobi coordinate ξ_i where the center of mass motion is separated. To describe the 3 → 3 scattering, we employ the hyperspherical oscillator basis which is the eigenfunction of a (3A - 3) dimensional harmonic oscillator, i.e. six dimensional HO for three-body case, with the frequency $\hbar\omega$ in the hyperspherical coordinates. The hyperspherical oscillator basis is defined as

$$
\begin{aligned}
|\kappa\Gamma\rangle \equiv |\kappa K\gamma\rangle &\equiv \langle\vec{\rho}\,|\kappa K((l_1 l_2)L(s_1 s_2)S)J(t_1 t_2)T\rangle \\
&= \mathcal{R}_{\kappa K}(\rho)\mathcal{Y}_{K\gamma}(\Omega_5),
\end{aligned}
$$

(4.6)

where $\mathcal{Y}_{K\gamma}(\Omega_5)$ is the hyperspherical function characterized by the set of quantum numbers $\gamma \equiv \{l_1, l_2, L, s_1, s_2, S, t_1, t_2, T\}$, κ is the oscillator principal quantum

number, l_1 and l_2 are the relative orbital momenta. The s_1, s_2 (t_1, t_2) is intermediate spin (isospin) couplings. The quantum numbers L, S and T specify the total orbital angular momentum, spin and isospin of the system. The L and S coupled to the total angular momentum J. The hyperradial oscillator function is defined as

$$\mathcal{R}_{\kappa K}(\rho) \equiv \mathcal{R}_\kappa^\mathcal{L}(\rho) = \rho^{-5/2} r_{\kappa K}(\rho), \tag{4.7}$$

$$r_{\kappa K}(\rho) \equiv r_\kappa^\mathcal{L}(\rho) = (-1)^\kappa \sqrt{\frac{2\kappa}{\Gamma(\kappa + \mathcal{L} + \frac{3}{2})}} \rho^{\mathcal{L}+1} e^{\frac{\rho^2}{2}} L_\kappa^{\mathcal{L}+\frac{1}{2}}(\rho^2), \tag{4.8}$$

where $\mathcal{L} = K + \dfrac{3}{2}$ for three-body system and the hyperspherical harmonics spin-isospin function is defined as

$$\mathcal{Y}_{K\gamma}(\Omega_5) \equiv \mathcal{Y}_\Gamma^{KLSJT}(\Omega_5, \vec{\chi}) = P_K^{l_1,l_2}(\beta) \mathcal{Y}_{l_1 l_2 LST}^{JM}(\widehat{\xi}_1, \widehat{\xi}_2, \vec{\chi}), \tag{4.9}$$

which is expressed detail in Appendix F. The Γ channel account for all possible quantum numbers for three-body system,

$$\Gamma \equiv \{K\gamma\} \equiv \{K, l_1, l_2, L, s_1, s_2, S, t_1, t_2, T\}, \tag{4.10}$$

which is consistent with the given values of K, L, S, J, T. The Eq. (4.6) to (4.8) define the eigenfunctions of the 3-body Schrodinger equation. The hyperspherical oscillator basis in Eq. (4.6) is orthonormalized

$$\langle \kappa \Gamma | \kappa' \Gamma' \rangle_\Omega \equiv \langle \kappa KLSJT | \kappa' K'L'S'J'T' \rangle_\Omega = \delta_{\kappa\kappa'} \delta_{\Gamma\Gamma'}, \tag{4.11}$$

where $\langle \; \rangle_\Omega$ indicates the evaluation of the spin-isospin traces and the integration over the hyperspherical variables. The total wave function of the system characterized by the total energy E and other quantum numbers α can be expanded in the hyperspherical oscillator function series

$$\Psi = |E\alpha\rangle$$

$$= \sum_{\kappa\Gamma} \langle \kappa\Gamma | E\alpha \rangle |\kappa\Gamma\rangle \equiv \sum_{\kappa KLSJT} \langle \kappa KLSJT | E\alpha \rangle |\kappa KLSJT\rangle, \tag{4.12}$$

and the Schrodinger equation takes the form

$$\sum_{\kappa'K'L'S'J'T'} \langle \kappa KLSJT| H - E |\kappa'K'L'S'J'T'\rangle$$

$$\times \langle \kappa'K'L'S'J'T'|E\alpha\rangle = 0.$$

(4.13)

The wave function $\langle \kappa'K'L'S'J'T'|E\alpha\rangle \equiv a_{\kappa K}(E)$ in the hyperspherical oscillator representation (OR) which is a solution of an infinite set of algebraic equations can be labeled by the principle quantum number κ or the number of oscillator quanta

$$N = 2\kappa + K = 2\kappa + \mathcal{L} - \frac{3}{2}.$$

(4.14)

Generally the Hamiltonian matrix elements is infinite. We split the complete infinite oscillator basis space into two parts: internal part and external part. For internal subspace specified by harmonic oscillator functions with $N \equiv 2n + l \leq N_{max}$ where the truncated Hamiltonian $H = T + V$ is used, we compute the eigenvalues of our system within the framework of NCSM approach using Jacobi formalism (see in Chap. II). In an extension of the finite NCSM Hamiltonian to continuum using J-Matrix(SS-HORSE) formalism, we consider only the kinetic energy matrix elements in the hyperspherical oscillator basis. The external subspace is specified by hyperspherical oscillator functions with $N \equiv 2\kappa + K > N_{\max}$ where the Hamiltonian $H = T$ is used. The free Schrodinger equation can be written in terms of maximum number of oscillator quanta $N_{\max}$ as

$$\sum_{N'_{\max}\Gamma'} \langle N_{\max}\Gamma| T - E |N'_{\max}\Gamma'\rangle \langle N'_{\max}\Gamma'|E\alpha\rangle = 0.$$

(4.15)

The kinetic energy matrix is diagonal with respect to the Γ and Γ' and tridiagonal with respect to κ and κ'. The non-zero KE matrix elements are increasing linearly with the principal quantum number κ or with the model space truncation $N_{\max}$. The tridiagonal KE matrix is

$$\langle N_{\max}\Gamma|\,T\,|N'_{\max}\Gamma'\rangle = \delta_{\Gamma\Gamma'}\Big[\,\langle N_{\max}-2|\,T\,|N'_{\max}\rangle + \langle N_{\max}|\,T\,|N'_{\max}\rangle$$

$$+\,\langle N_{\max}+2|\,T\,|N'_{\max}\rangle\,\Big]$$

$$=\frac{\hbar\omega}{2}\delta_{\Gamma\Gamma'}\Big[(N_{\max}+3)\delta_{N_{\max},N'_{\max}}$$

$$-\frac{1}{2}\sqrt{\Big(N_{\max}-\mathcal{L}+\frac{3}{2}\Big)\Big(N_{\max}+\mathcal{L}+\frac{5}{2}\Big)} \qquad (4.16)$$

$$\times\,\delta_{N_{\max}-2,N'_{\max}}$$

$$-\frac{1}{2}\sqrt{\Big(N_{\max}-\mathcal{L}+\frac{7}{2}\Big)\Big(N_{\max}+\mathcal{L}+\frac{9}{2}\Big)}$$

$$\times\,\delta_{N_{\max}+2,N'_{\max}}\Big].$$

By substituting Eq. (4.16) in Eq. (4.15), the Schrodinger equation becomes the form of three-term recurrence relation (TRR),

$$\langle N_{\max}-2|T\,|N'_{\max}\rangle\,a^{ass}_{N_{\max}-2,\mathcal{L}}(E) + \langle N_{\max}|\,T-E\,|N'_{\max}\rangle\,a^{ass}_{N_{\max}\mathcal{L}}(E)$$
$$+\,\langle N_{\max}+2|\,T\,|N'_{\max}\rangle\,a^{ass}_{N_{\max}+2,\mathcal{L}}(E) = 0. \qquad (4.17)$$

This Eq. (4.17) is a second order finite-difference equation. It has two independent solutions for the free Schrodinger equation in the hyperspherical OR which can be utilized in the case of arbitrary $\mathcal{L}$ (integer and half integer). The asymptotic wave function in the oscillator representation $a^{ass}_{N_{\max}\mathcal{L}}(E)$ is an arbitrary solution of Eq. (4.17), which is a superposition of the fundamental regular $S_{N_{\max}\mathcal{L}}(E)$ and irregular $C_{N_{\max}\mathcal{L}}(E)$ solutions,

$$a^{ass}_{N_{\max}\mathcal{L}}(E) = \langle N_{\max}\Gamma|E\alpha\rangle = \cos\delta_{\mathcal{L}}\,\mathrm{S}_{\mathrm{N}_{\max}\mathcal{L}}(\mathrm{E}) + \sin\delta_{\mathcal{L}}\,\mathrm{C}_{\mathrm{N}_{\max}\mathcal{L}}(\mathrm{E}), \quad (4.18)$$

where $\delta_{\mathcal{L}}$ is the scattering phase shift. The regular solution of Eq. (4.17) is the hyperradial momentum-space oscillator function,

$$S_{N_{\max}\mathcal{L}}(E) = \sqrt{\frac{(N_{\max} - \mathcal{L} + \frac{3}{2})!}{\lambda\,\Gamma(\frac{N_{\max}}{2} + \frac{\mathcal{L}}{2} + \frac{9}{4})}}\; q^{\mathcal{L}+1}\; e^{-\frac{q^2}{2}} L^{\mathcal{L}+\frac{1}{2}}_{(N_{\max}-\mathcal{L}+\frac{3}{2})/2}(q^2), \quad (4.19)$$

where $L^{\mathcal{L}+\frac{1}{2}}_{\kappa}(x)$ is the associated Laguerre polynomial, $\lambda = \sqrt{\frac{m\omega}{\hbar}}$ is the oscillator length. The irregular solutions are more complicated and can be generally expressed through Tricomi function $\Psi(a, c; x)$ (in terms of special functions).

$$C^{(\pm)}_{N_{\max}\mathcal{L}}(E) = \frac{1}{\pi\sqrt{\lambda}}\sqrt{(N_{\max} - \mathcal{L} + \frac{3}{2})!\,\Gamma(\frac{N_{\max}}{2} + \frac{\mathcal{L}}{2} + \frac{9}{4})}\; q^{\mathcal{L}+1}\; e^{\frac{q^2}{2}}$$
$$\quad (4.20)$$
$$\times\, e^{\mp i\pi(\mathcal{L}+\frac{1}{2})}\Psi(\frac{N_{\max}}{2} + \frac{\mathcal{L}}{2} + \frac{9}{4}, \mathcal{L} + \frac{3}{2}; e^{\mp i\pi}q^2),$$

$$C_{N_{\max}\mathcal{L}}(E) = \frac{1}{2}\Big(C^{(+)}_{N_{\max}\mathcal{L}}(E) + C^{(-)}_{N_{\max}\mathcal{L}}(E)\Big). \quad (4.21)$$

The wave function in the oscillator representation $a_{N\mathcal{L}}(E)$ in the internal subspace can be expressed through the external solution $a^{ass}_{N+2,\mathcal{L}}(E)$ in the asymptotic subspace as follow

$$a_{N\mathcal{L}}(E) = G_{N,N_{max}}(E)T^{\mathcal{L}}_{N_{max},N_{max}+2}\; a^{ass}_{N_{max}+2,\,\mathcal{L}}(E). \quad (4.22)$$

To be consistent in notation we need to introduce a bra-ket notation and in that case we will define the $a_{N\mathcal{L}}(E)$ as

$$\langle N\Gamma|E\alpha\rangle = \langle N\Gamma|\,G\,|N_{\max},\Gamma'\rangle\,\langle N_{\max},\Gamma'|\,T\,|N_{\max}+2,\Gamma'\rangle$$
$$\quad (4.23)$$
$$\times\,\langle N_{\max}+2,\Gamma'|E\alpha\rangle\,,$$

where $N = N_0, N_0 + 2, ..., N_{max}$. N_{max} is the maximal total quanta of many-body oscillator states. In our case, $N^{tot}_{max} = N_{max} + N_0 = N_{max}$. The matrix elements,

$$G_{NN'}(E) = -\sum_{\nu'=0}^{N} \frac{\langle N|\nu'\rangle \langle \nu'|N'\rangle}{E_{\nu'} - E}, \tag{4.24}$$

are described through the NCSM eigenenergies $E_{\nu'}$ and eigenvectors $\langle N|\nu\rangle$ of truncated Hamiltonian to the internal subspace. Only one diagonal matrix element

$$G_{N_{\max}N_{\max}}(E) = -\sum_{\nu=0}^{N_{\max}} \frac{\langle N_{\max}|\nu\rangle^2}{E_\nu - E}, \tag{4.25}$$

is responsible for the calculation of phase shifts. The scattering phase shifts can be derived through the matching condition where $N = N_{\max}$ as follow

$$a_{N_{\max}\mathcal{L}}(E) = a_{N_{\max}\mathcal{L}}^{ass}(E). \tag{4.26}$$

Substitution Eq. (4.22) in Eq. (4.26),

$$G_{N_{\max}N_{\max}}(E)\, T_{N_{\max},N_{\max}+2}^{\mathcal{L}}\, a_{N_{\max}+2,\,\mathcal{L}}^{ass}(E) = a_{N_{\max}\mathcal{L}}^{ass}(E), \tag{4.27}$$

$$G_{N_{\max}N_{\max}}(E)T_{N_{\max},N_{\max}+2}^{\mathcal{L}}\big(\cos\delta_{\mathcal{L}}\,\mathrm{S}_{N_{\max}+2,\,\mathcal{L}}(\mathrm{E}) + \sin\delta_{\mathcal{L}}\,\mathrm{C}_{N_{\max}+2,\,\mathcal{L}}(\mathrm{E})\big) \tag{4.28}$$
$$= \cos\delta_{\mathcal{L}}\mathrm{S}_{N_{\max}\mathcal{L}}(\mathrm{E}) + \sin\delta_{\mathcal{L}}\mathrm{C}_{N_{\max}\mathcal{L}}(\mathrm{E}),$$

$$\tan\delta_{\mathcal{L}}(\mathrm{E}) = -\frac{\mathrm{S}_{N_{\max}\mathcal{L}}(\mathrm{E}) - \mathrm{G}_{N_{\max}N_{\max}}(\mathrm{E})T_{N_{\max},N_{\max}+2}^{\mathcal{L}}\mathrm{S}_{N_{\max}+2,\,\mathcal{L}}(\mathrm{E})}{\mathrm{C}_{N_{\max}\mathcal{L}}(\mathrm{E}) - \mathrm{G}_{N_{\max}N_{\max}}(\mathrm{E})T_{N_{\max},N_{\max}+2}^{\mathcal{L}}\mathrm{C}_{N_{\max}+2,\,\mathcal{L}}(\mathrm{E})} \tag{4.29}$$

Note that the basis (4.6) is applicable for the calculation of three-body decays and not suitable for the calculation of interaction matrices. We remind here that the matrix elements of the two-body potentials V_{nn} and V_{nY} are computed in the basis

$$|nlsjt\rangle = |n_1l_1s_1j_1t_1, n_2l_2s_2j_2t_2 : JT\rangle$$
$$= |(n_{nn}l_{nn}s_{nn}j_{nn}t_{nn}, n_Yl_Ys_Yj_Yt_Y)JT\rangle. \tag{4.30}$$

Supposing that the basis functions (4.6) and (4.30) are specified by the same number

of oscillator quanta N, i.e, when the total oscillator quanta $2n_1 + l_1 + 2n_2 + l_2 = 2\kappa + K$ where κ is the principle quantum number for the hyper-radial, the extension of the kinetic energy matrix can be performed in the model space characterized by $2\kappa + K > N_{\max}$ $(2\kappa + K \geq N_{\max} + 2)$ to describe the external subspace. We do not need to do any transformations from NCSM jacobi-coordiante HO basis to hyperspherical coordinate HO basis since we could directly use the energies obtained from NCSM calculations to compute the $3 \rightarrow 3$ scattering phase shifts.

4.3.1 Minimum Approximation

The complete set of HH basis includes an infinite number of basis states with hypermomenta $K \geq K_{min}$ where K_{min} is the minimal hypermomentum consistent with the Pauli principle for a given nucleus. For practical calculations, the HH basis needs to be limited. We impose the minimum approximation of hypershpherical harmonic approach to take only HH basis with K_{min} for the Λnn democratic decay channel.

The two-body subsystems in Λnn system are assumed to be S wave states $(l_1 = l_2 = 0)$ and the minimum hypermomentum (the lowest angular momentum in the relative coordinate system) is

$$K_{min} = 0. \tag{4.31}$$

In the case of no sub-bound Λnn system, the HH states with large value of hypermomentum K are insignificant due to high centrifugal barrier $\mathcal{L}(\mathcal{L}+1)/\rho^2$, where ρ is hyper radius with the mass scaled Jacobi coordinates. Therefore, the kinetic energy extension to the NCSM is performed only in HH basis with hyperspherical momentum $K_{min} = 0$.

4.3.2 SS-HORSE Approach

A direct HORSE extension of computationally demanding NCSM calculations is impracticable. The Eq. (4.29) includes a sum over all possible eigenstates, i.e., over millions of states in modern NCSM computations. A calculation of a large number of many-body eigenstates is too computationally expensive and it is hard to obtain an adequate accuracy of the final sum in Eq. (4.29). To overcome these
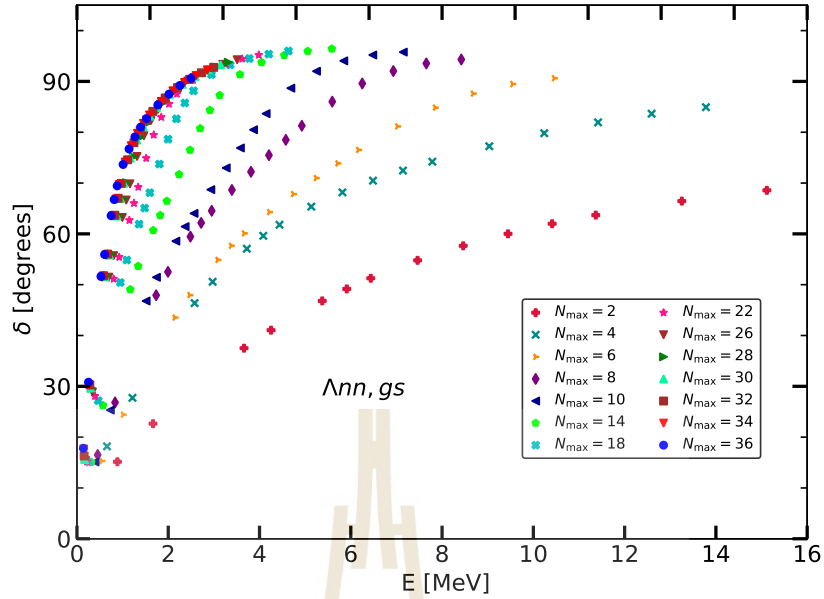
Figure 4.2 $3 \rightarrow 3$ scattering phase shifts obtained directly from the NCSM eigenstates using Eq. (4.32).

problems, we apply the SS-HORSE approach which computes the scattering phase shift at the eigenenergies $E_\nu > 0$ obtained directly from NCSM calculation. The Eq. (4.29) is reduced to

$$\tan \delta_{\mathcal{L}}(\mathrm{E}_\nu) = -\frac{\mathrm{S}_{\mathrm{N_{max}}+2, \mathcal{L}}(\mathrm{E}_\nu)}{\mathrm{C}_{\mathrm{N_{max}}+2, \mathcal{L}}(\mathrm{E}_\nu)}. \tag{4.32}$$

Generally speaking, a NCSM eigenstate E_ν defines all the properties of a nearby resonant state. So we calculate the $3 \rightarrow 3$ scattering phase shifts $\delta_{\mathcal{L}}(E_\nu)$ at these energies. We set $N_{\max}^{tot} = N_{\max}$ since the number of minimum HO quanta $N_0 = 0$. Then, one can use asymptotic expressions for $S_{N_{\max}+2, \mathcal{L}}(E_\nu)$ and $C_{N_{\max}+2, \mathcal{L}}(E_\nu)$ at large $N_{\max}$ when we calculated the NCSM calculations with even $N_{\max}$ for even parity $\frac{1}{2}^+$ state. The computed scattering phase shifts covering the NCSM eigenenergies from Figure 3.1 are presented in Figure 4.2.

We can see the phase shifts pattern which is going to be convergent with the increasing of model space size $N_{\max}$. The phase shifts at small values of $N_{\max}$ lie in the wide range of energy as the obtained Λnn ground-state energies spread widely and lead to outside the resonance region. When $N_{\max}$ increases, the obtained Λnn ground-state energies converge to lower values and
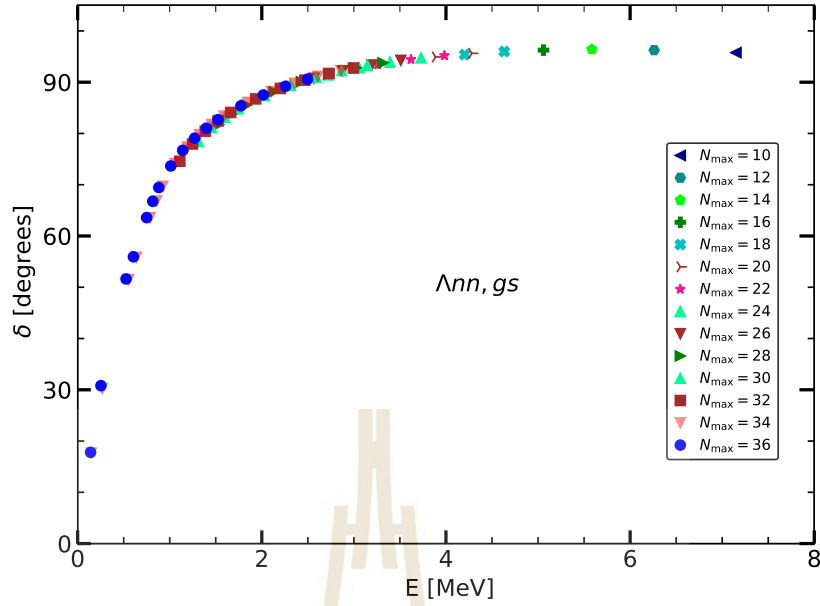
Figure 4.3 $3 \to 3$ scattering phase shifts obtained from selected NCSM eigenstates for scattering amplitude parametrization.

the corresponding phase shifts shift to the resonance energies region. The first convergence of phase shifts is achieved at smaller energies with larger $N_{\max}$, almost the same results at $N_{\max} = 34$ and 36 MeV. It is required to pick the lowest eigenenergies for further phase shift or scattering amplitude parametrization. There is no single rule for the selection of eigenenergies. We choose a set of eigenenergies from $N_{\max} = 10-36$ which produces the phase shifts lying on or close the common curve. The selected energy values are shown by blue shaded area in Figure 3.1. Their resulting SS-HORSE phase shifts in Figure 4.3 become a single smooth curve. We note that Eq. (4.32) can be used for scattering channels of any type.

In the low energy region of $q \to 0$, the phase shift behaves as $\delta \sim q^{2\mathcal{L}+1}$. In our case, $\mathcal{L} = \frac{3}{2}$ (half integer). The computed phase shift $\delta_{\mathcal{L}}(E) \sim q^4$ is an even function of q. Its expansion in Taylor series of even powers of $\sqrt{E} \sim q$ contradicts the symmetry properties of S-matrix. Apparently, S-Matrix symmetry is broken for all the systems having odd number of particles with half integer $\mathcal{L}$. Therefore, we instead compute the SS-HORSE low-energy scattering amplitude for the purpose of extracting the resonance parameters from scattering amplitude parametrization.

The SS-HORSE scattering amplitude $f_{\mathcal{L}}(E_\nu)$ is calculated through the standard formula as

$$f_{\mathcal{L}}(E_\nu)q = \frac{1}{(\cot\delta_{\mathcal{L}}(\mathrm{E}_\nu) - \mathrm{i})}. \tag{4.33}$$

The values of $\left|f_{\mathcal{L}}(E_\nu)q\right|^2$ at the respective set of phase shifts in Figure 4.3 are shown by solid symbols in Figure 4.4. Next section, we extrapolate the low energy scattering amplitudes on a larger energy interval using parametrizations of $\left|f_{\mathcal{L}}(E_\nu)q\right|^2$ and extract the resonance energy and width from fitting.

4.4   Parametrization of Scattering Amplitude

We parameterize the scattering amplitude in the method proposed in Ref. (Cho et al., 1993) for the case of resonance scattering on the basis of the scattering and resonance theory. In general, the resonance state is related with the pole of the scattering amplitude located on the second energy sheet at $E_p = E_r + i\frac{\Gamma}{2}$. When the resonance is not sharp, the resonance pole on scattering amplitude is undetermined and the contribution of non-resonant scattering amplitude becomes comparable with resonance one. In this case, non-resonant background needs to be taken into the resonance part. The sum of potential scattering (non-resonant background) and resonance contribution leads to a good approximation to exhibit the better resonance energy and width. The scattering amplitude may be parametrized as

$$F(E)q = e^{i\delta_0(E)}\sin\delta_0(\mathrm{E}) + \frac{-\Gamma/2}{\mathrm{E} - \mathrm{E_r} + \mathrm{i}\Gamma/2}\mathrm{e}^{2\mathrm{i}\delta_0(\mathrm{E})}, \tag{4.34}$$

where $\delta_0(E)$ is the potential scattering phase shift, depending on the energy E.

The real and imaginary part of the above complex-valued function $F(E)q$ can be written respectively as

$$ReF(E)q = \frac{\Gamma(-E + E_r)\cos 2\delta_0(\mathrm{E}) - \Gamma^2\sin 2\delta_0(\mathrm{E})}{\Gamma^2 + 4(E - E_r)^2}, \tag{4.35}$$
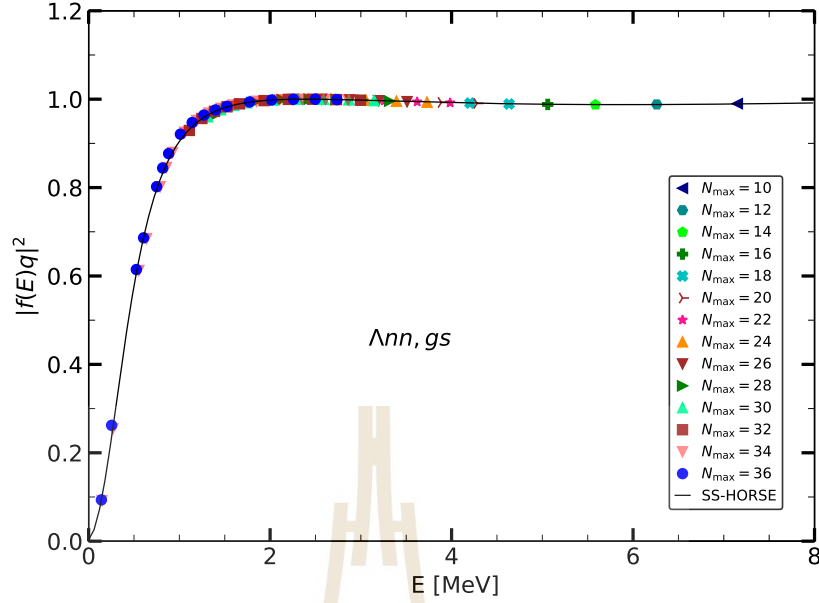
Figure 4.4 The scattering amplitude function $\left|f_{\mathcal{L}}(E_\nu)q\right|^2$ using Eq. (4.33) obtained from NCSM eigenstates (symbol). The solid line shows the parametrization of scattering amplitude using Eq. (4.34).

$$ImF(E)q = \frac{\Gamma^2\cos 2\delta_0(\mathrm{E}) + 2(\mathrm{E_r} - \mathrm{E})\sin 2\delta_0(\mathrm{E})}{\Gamma^2 + 2(E - E_r)^2}. \tag{4.36}$$

We perform minimization fit to both real and imaginary parts of the objective function

$$\Xi = \sqrt{\sum_\nu \left[F(E)q - f_{\mathcal{L}}(E_\nu)q\right]^2}, \tag{4.37}$$

and the background phaseshift form is chosen arbitrarily which may ensure $3 \rightarrow 3$ scattering phase shift $\delta \sim q^4$ in the low energy limit ($E \rightarrow 0$). The fitting to the SS-HORSE result $\left|f_{\mathcal{L}}(E_\nu)q\right|^2$ by the function $\left|F(E)q\right|^2$ leads the $\delta_0(E)$ to the form

$$\delta_0(E) = a_0 + a_2(\sqrt{E})^2 + a_4(\sqrt{E})^4, \tag{4.38}$$

with the adjustable parameters $a_0 = 1.856$, $a_2 = -0.014$ MeV^{-1}, $a_4 = 2.959$ $\times 10^{-4}$ MeV^{-2}. The resonance energy and width are extracted, $E_r = 0.124$ MeV and $\Gamma = 1.161$ MeV from the best fit to the data. The parametrization of the

scattering amplitude $|f_{\mathcal{L}}(E_\nu)q|^2$ with this selection of eigenstates is presented in Figure 4.4.

As we can see in Figure 4.2, the states with very smaller HO frequencies $\hbar\omega$ and large model space truncation $N_{\max}$ have very small energies. The selection of the NCSM energy points with very small $\hbar\omega$ may not very likely fulfill the condition for UV convergence. According to Table D.1, the eigenenergies should be calculated at approximate $\hbar\omega$ and $N_{\max}$ depending on the UV cutoff $\Lambda_{\mathrm{UV}} = 1200$ MeV for three-body system. We can see that $\hbar\omega$ depends on model space truncations $N_{\max}$ and decreases when $N_{\max}$ increases. But, within the SS-HORSE analysis, we can use all NSCM eigenstates forming a common curve to include scattering amplitudes from larger energy interval in our fitting, which enhance the accuracy of the fitting parameters.

Our results are in a good agreement with those in Ref. (Filikhin et al., 2016; Gibson and Afnan, 2019) and lies within the estimated range of the location and width of a Λnn pole (Schäfer et al., 2021). We look forward to the results of both Λnn bound and resonance states from ongoing experiment (E12-17-003) at Jefferson Lab (JLab) (Tang et al.,) in order to gain new perspective on Λn interactions. Such a Λnn resonance, if any, can be used to constrain the Λn interaction in the calculation of few-body Λ hypernuclei.

CHAPTER V

CONCLUSIONS

In this work, we performed the no-core shell model calculations for s-shell light hypernuclei ${}^3_\Lambda H$, ${}^4_\Lambda H$ and ${}^3_\Lambda He$ using a family of chiral NNLO$_{\text{sim}}$ nucleon-nucleon interactions and a fixed chiral LO hyperon-nucleon interaction. The standard IR extrapolation technique are first applied in the hypernuclear NCSM calculations. It reduces the errors concerning with selection procedure of which data points are actually need to include in fitting. We have estimated the uncertainty in the predicted three- and four-body hypernuclear binding energy due to the model uncertainty of the NN interaction. We got the precious information for very limited YN physics by studying the hypernuclear systems with also study of NN sensitivity. When we go to the next orders of YN interaction in CEFT, we need to come up with more observables to constrain more parameters for NLO. As a consequence of our finding of small sensitivity of A=3 and 4 hypernuclear binding energy found with the NNLO$_{\text{sim}}$ family of interactions, one may claim that the spectra of light hypernuclei provides the important constraints on the hyperon-nucleon interaction models. Present method can be employed to study the systematic uncertainty of p-shell hypernuclei using the M-scheme basis.

We have performed ab initio no-core shell model calculations for the Λnn system $(J^\pi = 1/2^+, T = 1)$ without tuning the strength of realistic NN and YN potentials at various N_{max} and $\hbar\omega$ values with full inclusion of ΛN-ΣN coupling, and found that no bound state exists. To look for resonance states of the Λnn, we have applied the SS-HORSE method which permits calculating phase shift by using the NCSM eigenenergy values alone. From the minimization fit of scattering amplitude by the complex function $F(E)q$ which expresss both resonance and potential scattering region, we derive a Λnn resonant state at energy $E_r = 0.124$ MeV and width $\Gamma = 1.161$ MeV. Further theoretical studies and experimental searches for Λnn resonances would be of great benefit of constraining Λn interactions.

5.1 future work

In the future, we intend to perform the uncertainties quantification of A=5 and 6-body hypernuclear binding energies to get more observables as additional constraints on YN interaction. Moreover, we plan to carry out the SS-HORSE calculations for four particles Λnnn system, also studying the S-matrix poles related to unbound Λnnn state.
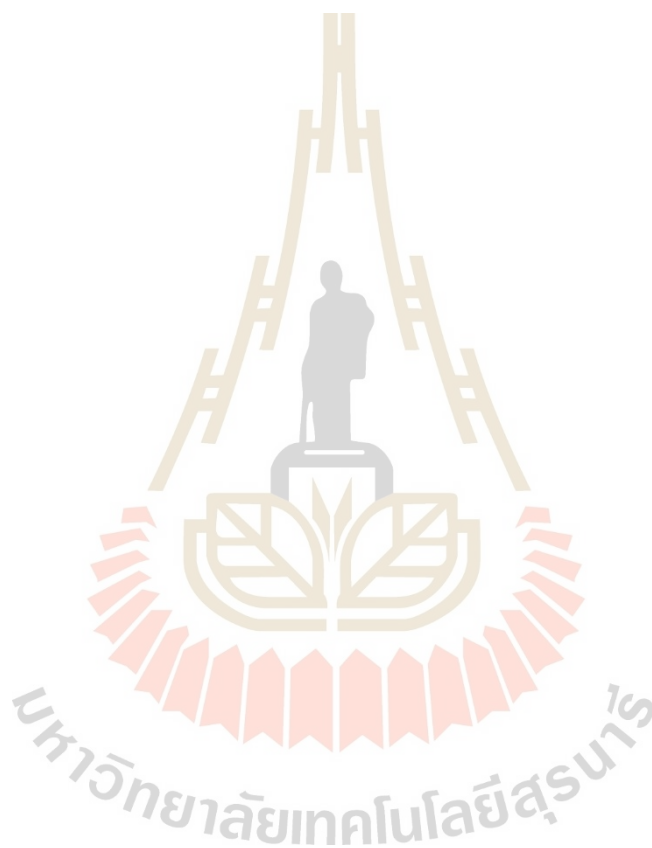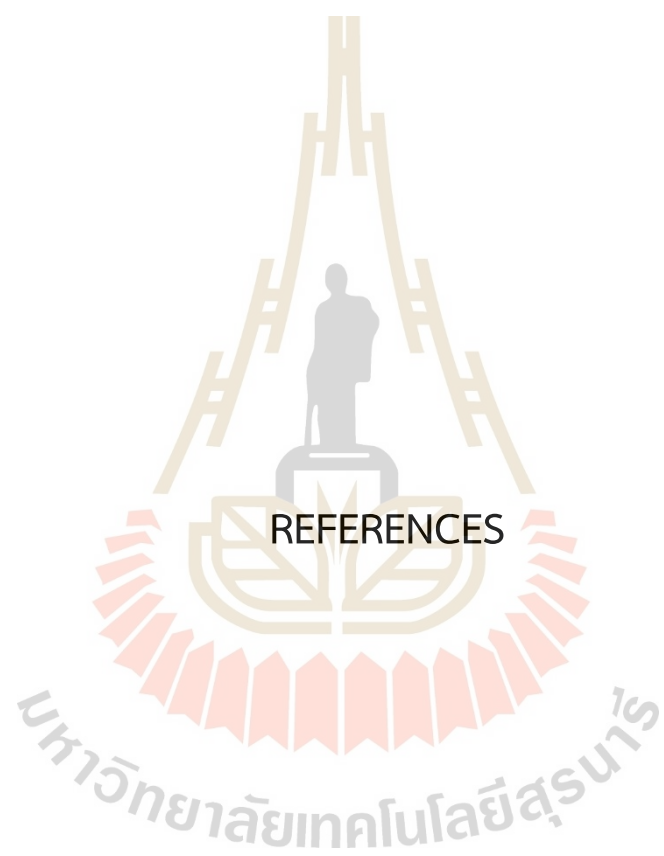
REFERENCES

REFERENCES

Acharya, B., Carlsson, B. D., Ekström, A., Forssén, C., and Platter, L. (2016). Uncertainty quantification for proton–proton fusion in chiral effective field theory. *Physical Letter B, 760,* 584–589.

Afnan, I. R. and Gibson, B. F. (2015). Resonances in the Λnn system. *Physical Review C, 92*(5), 054608.

Ando, S.-I., Raha, U., and Oh, Y. (2015). Investigation of the nnΛ bound state in pionless effective theory. *Physical Review C, 92*(2), 024325.

Bang, J., Mazur, A., Shirokov, A., Smirnov, Y., and Zaytsev, S. (2000). P-matrix and j-matrix approaches: Coulomb asymptotics in the harmonic oscillator representation of scattering theory. *Annals of Physics, 280*(2), 299-335.

Belyaev, V., Rakityansky, S., and Sandhas, W. (2008). Three-body resonances Λnn and $\Lambda\Lambda$n. *Nuclear Physics A, 803*(3), 210–226.

Binder, S., Calci, A., Epelbaum, E., Furnstahl, R. J., Golak, J., Hebeler, K., Kamada, H., Krebs, H., Langhammer, J., Liebig, S., Maris, P., Meißner, U.-G., Minossi, D., Nogga, A., Potter, H., Roth, R., Skibiński, R., Topolnicki, K., Vary, J. P., and Witała, H. (2016). Few-nucleon systems with state-of-the-art chiral nucleon-nucleon forces. *Physical Review C, 93*(6), 044002.

Blokhintsev, L., Mazur, A., Mazur, I., Savin, D., and Shirokov, A. (2017). SS-HORSE method for studying resonances. *Physics of Atomic Nuclei, 80*(2), 226–236.

Carlsson, B. D., Ekström, A., Forssén, C., Strömberg, D. F., Jansen, G. R., Lilja, O., Lindby, M., Mattsson, B. A., and Wendt, K. A. (2016). Uncertainty analysis and order-by-order optimization of chiral nuclear interactions. *Physical Review X, 6*(1), 011019.

Cho, G.-C., Kasari, H., and Yamaguchi, Y. (1993). General theory of resonance scattering. *Progress of Theoretical Physics, 90,* 783–802.

Contessi, L., Barnea, N., and Gal, A. (2018). Resolving the Λ Hypernuclear Overbinding Problem in Pionless Effective Field Theory. *Physical Review Letter, 121*(10), 102502.

Coon, S. A., Avetian, M. I., Kruse, M. K. G., van Kolck, U., Maris, P., and Vary, J. P. (2012). Convergence properties of ab initio calculations of light nuclei in a harmonic oscillator basis. *Physical Review C, 86,* 054002.

Davis, D. H. (2005). 50 years of hypernuclear physics. I. The early experiments. *Nuclear Physics A, 754,* 3–13.

Downs, B. W. and Dalitz, R. H. (1959). Analysis of the Λ-Hypernuclear Three-Body Systems. *Physical Review, 114,* 593-602.

Ekström, A., Carlsson, B. D., Wendt, K. A., Forssén, C., Hjorth-Jensen, M., Machleidt, R., and Wild, S. M. (2015). Statistical uncertainties of a chiral interaction at next-to-next-to leading order. *Journal of Physics G, 42*(3), 034003.

Ekström, A., Carlsson, B. D., Wendt, K. A., Forssén, C., Jensen, M. H., Machleidt, R., and Wild, S. M. (2015). Statistical uncertainties of a chiral interaction at next-to-next-to leading order. *Journal of Physics G: Nuclear and Particle Physics, 42*(3), 034003.

Filikhin, I., Suslov, V., and Vlahovic, B. (2016). Λnn bound state with three-body potential. *EPJ Web Conferences, 113,* 08006.

Forssén, C., Carlsson, B. D., Johansson, H. T., Sääf, D., Bansal, A., Hagen, G., and Papenbrock, T. (2018). Large-scale exact diagonalizations reveal low-momentum scales of nuclei. *Physical Review C, 97*(3), 034328.

Furnstahl, R. J., Hagen, G., and Papenbrock, T. (2012). Corrections to nuclear energies and radii in finite oscillator spaces. *Physical Review C, 86,* 031301.

Furnstahl, R. J., Klco, N., Phillips, D. R., and Wesolowski, S. (2015). Quantifying truncation errors in effective field theory. *Physical Review C, 92*(2), 024005.

Garcilazo, H. and Valcarce, A. (2014). Nonexistence of a Λnn bound state. *Physical Review C, 89*(5), 057001.

Gibson, B. and Afnan, I. (2019). The Λn scattering length and the Λnn resonance. *AIP Conference Proceedings, 2130*(1), 020005.

Hildenbrand, F. and Hammer, H.-W. (2019). Three-Body Hypernuclei in Pionless Effective Field Theory. *Physical Review C, 100*(3), 034002. [Erratum: Phys.Rev.C 102, 039901 (2020)].

Htun, T. Y., Gazda, D., Forssén, C., and Yan, Y. (2021). Systematic Nuclear Uncertainties in the Hypertriton System. *Few Body System, 62*(4), 94.

Kamada, H., Miyagawa, K., and Yamaguchi, M. (2016). A Λnn three-body resonance. *EPJ Web of Conferences, 113*07004.

Kamuntavicius, G. P., Kalinauskas, R. K., Barrett, B. R., Mickevicius, S., and Germanas, D. (2001). The General harmonic oscillator brackets: Compact expression, symmetries, sums and Fortran code. *Nuclear Physics A, 695,* 191–201.

Le, H., Haidenbauer, J., Meißner, U.-G., and Nogga, A. (2020). Jacobi no-core shell model for p-shell hypernuclei. *The European Physical Journal A, 56*(12), 301.

Lonardoni, D., Gandolfi, S., and Pederiva, F. (2013). Effects of the two-body and three-body hyperon-nucleon interactions in Λ-hypernuclei. *Physical Review C, 87,* 041303.

Lurie, Y. A. and Shirokov, A. M. (2004). Loosely bound three body nuclear systems in the J matrix approach. *Annals Physics, 312,* 284–318.

Mazur, A. I., Shirokov, A. M., Mazur, I. A., Blokhintsev, L. D., Kim, Y., Shin, I. J., and Vary, J. P. (2019). Description of Continuum States within the No-Core Shell Model: Single-State HORSE Method. *Physics of Atomic Nuclei, 82*(5), 537–548.

Mazur, I., Shirokov, A., Mazur, A., and Vary, J. (2017). Description of resonant states in the shell model. *Physics of Particles and Nuclei, 48*(1), 84–89.

Navarro Pérez, R., Amaro, J. E., Ruiz Arriola, E., Maris, P., and Vary, J. P. (2015). Statistical error propagation in ab initio no-core full configuration calculations of light nuclei. *Physical Review C, 92*(6), 064003.

Nogga, A. (2013). Light hypernuclei based on chiral and phenomenological interactions. *Nuclear Physics A, 914,* 140–150.

Pérez, R. N., Amaro, J. E., and Arriola, E. R. (2015). Error analysis of nuclear forces and effective interactions. *Journal of Physics G: Nuclear and Particle Physics, 42*(3), 034013.

Polinder, H., Haidenbauer, J., and Meissner, U.-G. (2006). Hyperon-nucleon interactions: A Chiral effective field theory approach. *Nuclear Physics A, 779,* 244–266.

Schäfer, M., Bazak, B., Barnea, N., and Mareš, J. (2021). Nature of the Λnn $(J^\pi = 1/2^+, I = 1)$ and $_\Lambda^3\mathrm{H}^*(J^\pi = 3/2^+, I = 0)$ states. *Physical Review C, 103*(2), 2.

Shirokov, A., Mazur, A., Mazur, I., and Vary, J. (2016a). Shell Model States in the Continuum. *Physical Review C, 94*(6), 064320. [Erratum: Phys.Rev.C 98, 039901 (2018)].

Shirokov, A., Papadimitriou, G., Mazur, A., Mazur, I., Roth, R., and Vary, J. (2016b). Prediction for a four-neutron resonance. *Physical Review Letter, 117,* 182502. [Erratum: Phys.Rev.Lett. 121, 099901 (2018)].

Shirokov, A. M., Mazur, A. I., Mazur, I. A., Mazur, E. A., Shin, I. J., Kim, Y., Blokhintsev, L. D., and Vary, J. P. (2018). Nucleon-α Scattering and Resonances in ^{5}He and ^{5}Li with JISP16 and Daejeon16 NN interactions. *Physical Review C, 98*(4), 044624.

Tang, L., Garibaldi, F., Markowitz, P., Nakamura, S., Reinhold, J., and G.M., U. (JLab Hall A Collaboration), Extension request for E12- 17-003: Determining the unknown Λ-n interaction by investigating the Λnn resonance (2018). *Proposal to Jefferson Lab PAC 48.*

Wendt, K. A., Forssén, C., Papenbrock, T., and Sääf, D. (2015). Infrared length scale and extrapolations for the no-core shell model. *Physical Review C, 91*(6), 061301.

Wirth, R., Gazda, D., Navrátil, P., Calci, A., Langhammer, J., and Roth, R. (2014). Ab Initio Description of p-Shell Hypernuclei. *Physical Review Letter, 113*(19), 192502.

Wirth, R., Gazda, D., Navrátil, P., and Roth, R. (2018). Hypernuclear No-Core Shell Model. *Physical Review C, 97*(6), 064315.

Yamany, H. A. and Fishman, L. (1975). J–matrix method: Extensions to arbitrary angular momentum and to Coulomb scattering. *Journal of Mathematical Physics, 16, 410*.

Zaitsev, S., Smirnov, Y., and Shirokov, A. (1998). True many-particle scattering in the oscillator representation. *Theoretical and Mathematical Physics, 117,* 1291–1307.
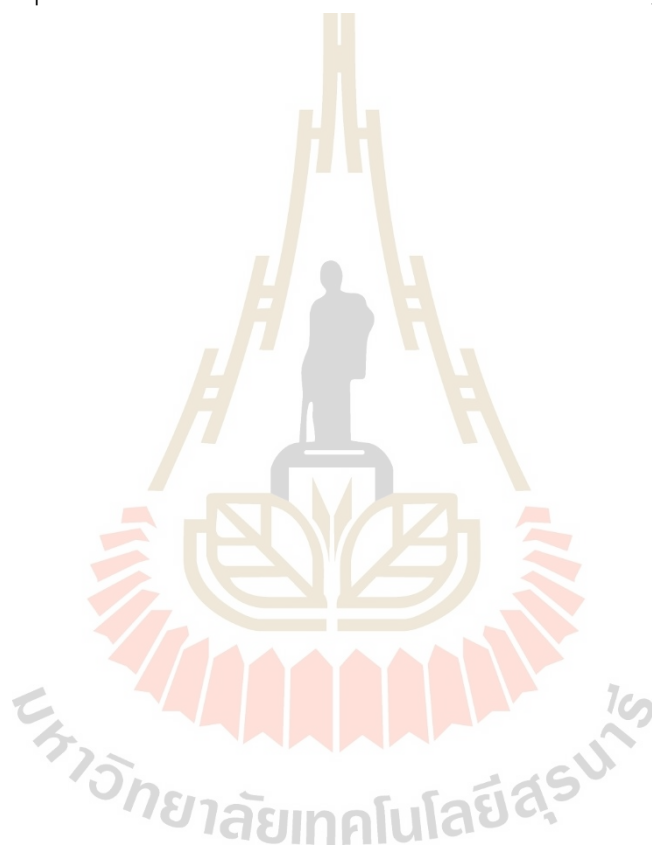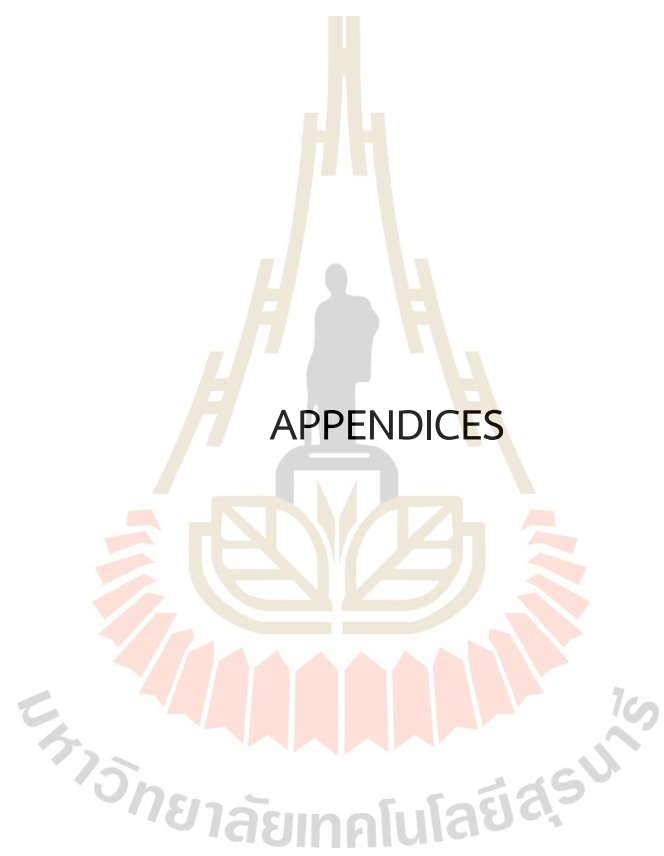
APPENDICES

APPENDIX A

BASIS ANTISYMMETRIZATION

The JT-coupled HO basis have to be antisymmetrized. We treat the hyperon as a distinguishable particles and exclude it from the antisymmetrization process. We assume the hyperon is A^{th} particle. The fully antisymmetrized basis of A-body system with strangeness can be obtained from doing the same procedure as in the purely nucleonic system using a Jacobi-coordinate HO basis. The fully antisymmetrization given by the exchanges of all $A-1$ nucleons can be obtained by diagonalization the antisymmetrizer in the basis (2.12). The antisymmetrization operator for (A-1) nucleon systems is given by

$$\mathcal{A}_{A-1} = \frac{1}{(A-1)!} \sum_{\pi} sgn(\pi)\mathcal{P}_{\pi}, \tag{A.1}$$

where $\mathcal{P}_{\pi}$ is the all permutation operators exchanging two nucleons. This antisymmetrizer act as an identity operator on the hyperon state. For the 3-body hypernuclear case, the action of antisymmetrizer in the two-nucleon state is very simple

$$\mathcal{A}_2 \left|(\alpha_1, \alpha_2)JT\right\rangle = \frac{1}{2}(1 - \mathcal{P}_{12})\left|(\alpha_1, \alpha_2)JT\right\rangle$$
$$= \frac{1}{2}\left[1 - (-1)^{l_1+s_1+t_1}\right]\left|(\alpha_1, \alpha_2)JT\right\rangle. \tag{A.2}$$

The permutation operator $\mathcal{P}_{12}$ exchanges the position of nucleon 1 and 2 in the $|\alpha_1\rangle \equiv |n_{NN}(l_{NN}s_{NN})j_{NN}t_{NN}\rangle$ two-nucleon state depending on the Jacobi coordinate $\vec{\xi_1}$ and does not make sense on $|\alpha_2\rangle \equiv |n_Y(l_Ys_Y)j_Yt_Y\rangle$ state depending on $\vec{\xi_2}$ coordinate between NN pair and a hyperon.

For the 4-body hypernuclear case, the antisymmetrizer needed for antisymmetrization of three nucleons states can be represented as

$$\mathcal{A}_3 = \frac{1}{3}[1 - 2\mathcal{P}_{23}]. \tag{A.3}$$

The result of Eq. (A.2) together with above antisymmetrizer in Eq. (A.3) is employed to initiate the iterative procedure of constructing the antisymmetrized basis for a larger number of particles, by adding one nucleon at a time. The calculations often require to represent basis states in terms of states of subclusters. A basis containing an antisymmetrized subcluster of three nucleons is

$$|N_{NNN}i_{NNN}J_{NNN}T_{NNN}\rangle \equiv |N_3 i_3 J_3 T_3\rangle \,, \tag{A.4}$$

where the quantum number i_3 distinguishes between different antisymmetric states with the same quantum numbers N_3, J_3, T_3. The basis state can be expanded in the states containing antisymmetrized subcluster of two nucleons and one nucleon as

$$|N_3 i_3 J_3 T_3\rangle = \sum_{N_2 i_2 J_2 T_2} \sum_{\alpha_2} \langle (N_2 i_2 J_2 T_2, \alpha_2) J_3 T_3 | N_3 i_3 J_3 T_3 \rangle$$
$$\times |(N_2 i_2 J_2 T_{NN}, \alpha_2) J_3 T_3\rangle \,, \tag{A.5}$$

where the state $|\alpha_2\rangle \equiv |\mathcal{N}_N \mathcal{L}_N \mathcal{J}_N\rangle$ corresponds to a 3rd nucleon. Note that the subscripts of the HO quantum numbers N, J, T refer to the number of nucleons and of the state $|\alpha_i\rangle$ refer to the Jacobi coordinates ξ_i. The matrix element in above equation is the coefficients of fractional parentage (cfp) which define the antisymmetric 3-body state in terms of antisymmetric 2-body states in relative motion with respect to the 3rd nucleon. We obtain these states by diagonalization of permutation operator in Eq. (A.3),

$$\langle (N_2' i_2' J_2' T_2', \alpha_2') J_3 T_3, \alpha_3, JT| \mathcal{P}_{23} |(N_2 i_2 J_2 T_2, \alpha_2, J_3 T_3, \alpha_3) JT\rangle$$

$$= \delta_N^{N'} \sum_{N_1 i_1 J_1 T_1} \sum_{\alpha_1} \langle (N_1' i_1' J_1' T_1', \alpha_1') J_2' T_2' | N_2' i_2' J_2' T_2' \rangle$$

$$\times \langle\langle n_2' l_2', n_1' l_1' | n_2 l_2, n_1 l_1 : L\rangle\rangle_{\frac{1}{3}} \tag{A.6}$$

$$\times (-1)^{T_2' + T_2 + J_1' + J_1} \langle (N_1 i_1 J_1 T_1, \alpha_1) J_2 T_2 | N_2 i_2 J_2 T_2 \rangle$$

$$\times \hat{T}_2' \hat{T}_2 \hat{j}_1' \hat{j}_1 \hat{j}_1' \hat{j}_2 \hat{J}_2' \hat{J}_2 \hat{K}^2 \hat{L}^2 \begin{Bmatrix} 1/2 & T_1 & T_2 \\ 1/2 & T_3 & T_2' \end{Bmatrix} \begin{Bmatrix} l_1' & l_2 & K \\ j_2 & j_1' & 1/2 \end{Bmatrix}$$

$$\times (-1)^{l_2'+l_2} \begin{Bmatrix} l_1 & l_2' & K \\ j_2' & j_1 & 1/2 \end{Bmatrix} \begin{Bmatrix} l_2' & l_1 & K \\ l_2 & l_1' & L \end{Bmatrix} \begin{Bmatrix} J_1 & j_1' & j_2' \\ j_1 & K & J_2' \\ J_2 & j_2 & J_3 \end{Bmatrix}.$$

The permutation operator $\mathcal{P}_{23}$ exchanges the position of nucleon 2 and 3 in the three-nucleon $|(N_2 i_2 J_2 T_2, \alpha_2) J_3 T_3\rangle$ state depending on the Jacobi coordinates $\vec{\xi}_1, \vec{\xi}_2$ and does not make sense on the $|\alpha_3\rangle \equiv |n_Y(l_Y s_Y) j_Y t_Y\rangle$ state depending on the $\vec{\xi}_3$ coordinate between NNN pair and a hyperon. The fully anti-symmetrized states (and eigenvalues = 0, 1) are only obtained when the complete block of intermediate states for J, T and N was included. The Harmonic Oscillator Brackets $\langle\langle n_2' l_2', n_1' l_1' | n_2 l_2, n_1 l_1 : L \rangle\rangle_{d=\frac{1}{(A-1)(A-3)}}$ follow the convention of Ref. (Kamuntavicius et al., 2001) and mediate the transformation between two coordinates. The resulting states for 4-body hypernucleus

$$|(N_3 i_3 J_3 T_3, \alpha_3) JT\rangle, \tag{A.7}$$

are antisymmetric with respect to exchanges of all nucleons.
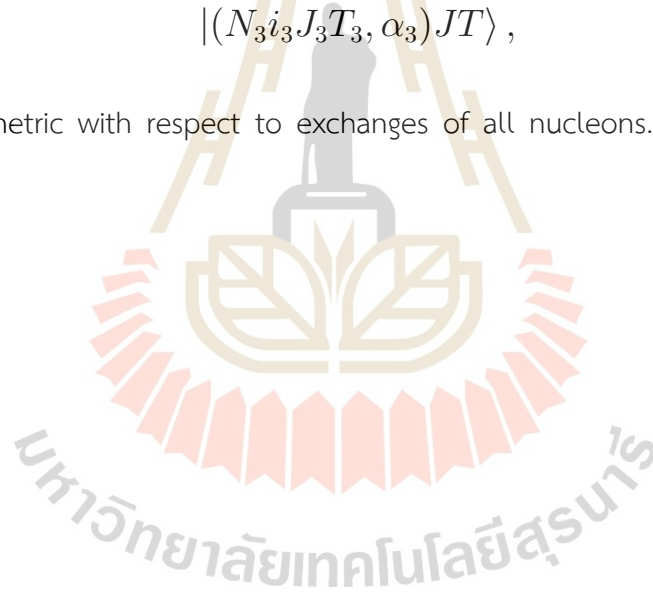
APPENDIX B

RECOUPLING COEFFICIENT

We here express the recoupling coefficient for the simple three-body case as an example. The three-body recoupling coefficient arising from coordinate transformation $(\vec{\xi_1}, \vec{\xi_2}$ to $\vec{\eta_2}, \vec{\eta_1}$) can be obtained through the jj coupling, ls coupling and spin coupling and isospin coupling. To be simplify, we use the index 1, 2 for two nucleons and index 3 for a hyperon in three body systems. The explicit expression for the three-body recoupling coefficients will be

$$\langle (n_{13}n_2(l_{13}s_{13})J_{13}(l_2s_2)I_2)J(T_{13}t_2)T | n_{12}n_3(l_{12}s_{12})J_{12}(l_3s_3)I_3)J(T_{12}t_3)T\rangle$$

$$= \langle n_{13}n_2|n_{12}n_3\rangle \langle (l_{13}s_{13})J_{13}(l_2s_2)I_2)J|(l_{12}s_{12})J_{12}(l_3s_3)I_3)J\rangle$$
$$\times \langle ((t_1t_3)T_{13}t_2)T|((t_1t_2)T_{12}t_3)T\rangle \tag{B.1}$$

Let us couple three isospin t_1, t_2 and t_3 to the total isospin T. There are two ways: (1) first t_1, $t_2 \to t_{12}$ and then t_{12}, $t_3 \to T$. (2) first t_2, $t_3 \to t_{23}$ and then t_{23}, $t_1 \to T$. The three isospin coupling can be expressed by 6-j symbols,

$$\langle ((t_1t_3)T_{13}t_2)T|((t_1t_2)T_{12}t_3)T\rangle = (-1)^{T_{13}+t_2+T_{12}+t_3}\hat{T}_{13}\hat{t}_2$$
$$\times \begin{Bmatrix} t_2 & t_1 & T_{12} \\ t_3 & T & T_{13} \end{Bmatrix}. \tag{B.2}$$

JJ coupling need to transform to LS coupling as

$$\langle (l_{13}S_{13})J_{13}(l_2s_2)I_2)J|(l_{12}S_{12})J_{12}(l_3s_3)I_3)J\rangle$$

$$= \sum_{LS} \langle (l_{13}S_{13})J_{13}(l_2s_2)I_2)J|((l_{13}l_2)L(S_{13}s_2)S)J\rangle$$
$$\times \langle ((l_{13}l_2)L(S_{13}s_2)S)J|((l_{12}l_3)L(S_{12}s_3)S)J\rangle \tag{B.3}$$
$$\times \langle ((l_{12}l_3)L(S_{12}s_3)S)J|(l_{12}s_{12})J_{12}(l_3s_3)I_3)J\rangle .$$

Transformation of the state jj coupling to ls coupling,

$$|(l_{13}S_{13})J_{13}(l_2s_2)I_2)J\rangle = \sum_{LS} |((l_{13}l_2)L(S_{13}s_2)S)J\rangle \begin{Bmatrix} l_{13} & S_{13} & J_{13} \\ l_2 & s_2 & I_2 \\ L & S & J \end{Bmatrix}. \text{(B.4)}$$

Coupling coefficient between jj and ls is given by 9j symbol.

$$\langle (l_{13}S_{13})J_{13}(l_2s_2)I_2)J|((l_{13}l_2)L(S_{13}s_2)S)J\rangle = \sum_{LS} \hat{J}_{13}\hat{I}_2\hat{L}\hat{S}$$

$$\times \begin{Bmatrix} l_{13} & S_{13} & J_{13} \\ l_2 & s_2 & I_2 \\ L & S & J \end{Bmatrix}. \quad \text{(B.5)}$$

Above JJ coupling coefficient become

$$\langle (l_{13}S_{13})J_{13}(l_2s_2)I_2)J|(l_{12}S_{12})J_{12}(l_3s_3)I_3)J\rangle$$

$$= \sum_{LS} \hat{J}_{13}\hat{I}_2\hat{J}_{12}\hat{I}_3\hat{L}^2\hat{S}^2 \langle ((l_{13}l_2)L(S_{13}s_2)S|(l_{12}l_3)L(S_{12}s_3)S\rangle$$

$$\times \begin{Bmatrix} l_{13} & S_{13} & J_{13} \\ l_2 & s_2 & I_2 \\ L & S & J \end{Bmatrix} \begin{Bmatrix} l_{12} & S_{12} & J_{12} \\ l_3 & s_3 & I_3 \\ L & S & J \end{Bmatrix}. \quad \text{(B.6)}$$

$$\langle ((l_{13}l_2)L(S_{13}s_2)S|(l_{12}l_3)L(S_{12}s_3)S\rangle = \langle (l_{13}l_2)L|(l_{12}l_3)L\rangle$$

$$\times \langle (S_{13}s_2)S|(S_{12}s_3)S\rangle. \quad \text{(B.7)}$$

The three spin coupling coefficient is also given by 6j symbol as

$$\langle (S_{13}s_2)S|(S_{12}s_3)S\rangle = (-1)^{S_{13}+s_2+S_{12}+s_3}\hat{S}_{13}\hat{S}_{12} \begin{Bmatrix} s_2 & s_1 & S_{12} \\ s_3 & S & S_{13} \end{Bmatrix}. \quad \text{(B.8)}$$

The general expression for three-body recoupling coefficient is

$$\langle (n_{13}n_2(l_{13}s_{13})J_{13}(l_2s_2)I_2)J(T_{13}t_2)T|(n_{12}n_3(l_{12}s_{12})J_{12}(l_3s_3)I_3)J(T_{12}t_3)T\rangle$$

$$= \hat{J}_{13}\hat{I}_2\hat{J}_{12}\hat{I}_3(-1)^{S_{13}+s_2+S_{12}+s_3\hat{S}_{13}+l_2+l_3+T_{13}+t_2+T_{12}+t_3}\sum_{LS}\hat{L}^2\hat{S}^2\hat{T}_{13}\hat{T}_{12}$$

$$\times \begin{Bmatrix} l_{13} & S_{13} & J_{13} \\ l_2 & s_2 & I_2 \\ L & S & J \end{Bmatrix} \begin{Bmatrix} l_{12} & S_{12} & J_{12} \\ l_3 & s_3 & I_3 \\ L & S & J \end{Bmatrix} \begin{Bmatrix} s_2 & s_1 & S_{12} \\ s_3 & S & S_{13} \end{Bmatrix} \begin{Bmatrix} t_2 & t_1 & T_{12} \\ t_3 & T & T_{13} \end{Bmatrix} \quad \text{(B.9)}$$

$$\times \langle n_{13}l_{13}n_2l_2L|n_{12}l_{12}n_3l_3L\rangle_{d=\frac{2m+m_3}{m_3}} .$$

The corresponding harmonic-oscillator brackets (HOBs) $\langle n_{13}l_{13}n_2l_2L|n_{12}l_{12}n_3l_3L\rangle_d$ can be calculated by filling the arrays of the binomial and trinomial coefficients. The code was based on the observation that all group-theoretical expressions can be represented as products or sums of products of binomial coefficients (Kamuntavicius et al., 2001). We directly use this general coordinate transformation technique for our three-body calculations.

APPENDIX C

BASIS DIMENSION

The model-space dimension of the Jacobi coordinate HO basis grows rapidly with the increasing of the model space size $N_{\max}$ and the number of particles in the system. Going to higher $N_{\max}$ in studying the entire NNLO$_{\text{sim}}$ family is computationally costly for heavier hypernuclei. In our calculation, the dimension for ground state of $^4_\Lambda He$ and $^4_\Lambda H$ at $N_{\max} = 20$ is 7.9×10^4 and, which is the highest limit that supercomputers can handle when employing NNN forces.
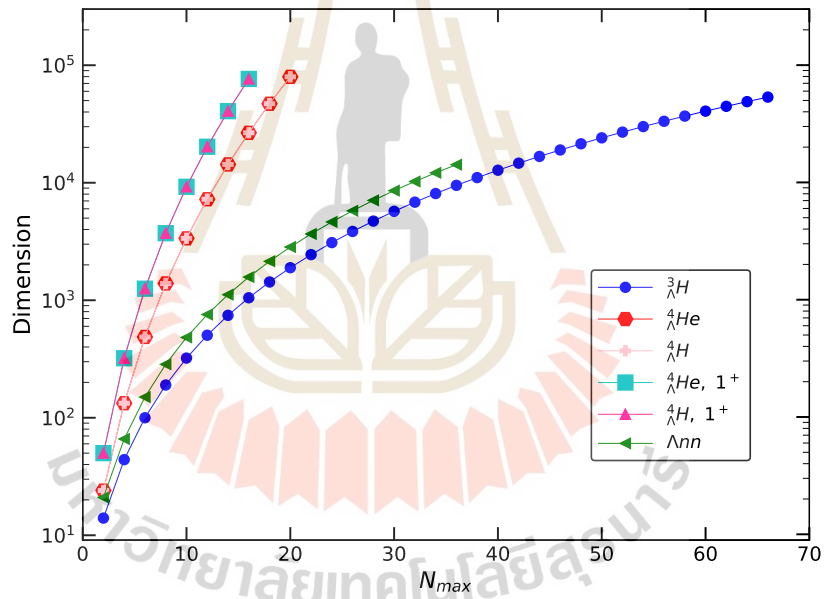
Figure C.1 Basis dimension of the full NCSM space as function of $N_{\max}$ for $^3_\Lambda H$, $^4_\Lambda H$, $^4_\Lambda He$ hypernuclei and a Λnn system.

All of computations were performed on resources provided by the Swedish National Infrastructure for Computing (SNIC) at C3SE (Chalmers) and NSC (Linköping). The Λnn computations were performed at SUT server.

APPENDIX D

IR LENGTH SCALE AND RELATED HO FREQUENCIES

The IR length scales L_{eff} for relevant hypernuclei are needed to perform IR extrapolation which can estimate the final result from small model spaces missing IR physics. The main idea to compute the infrared length scale is to equate the instrinsic kinetic energy of A fermions in the NCSM space to that of A fermions in a $(3A - 3)$-dimensional hyper-radial well. For this purpose, we firstly compute the eigenvalues of the kinetic energy for a $(3A - 3)$-dimensional hyper-radial well with an infinite wall at hyper radius ρ. The hyper-radial part of the noninteracting Hamiltonian is

$$-\left(\frac{\partial^2}{\partial^2\rho^2} - \frac{\mathcal{L}(\mathcal{L}+1)}{\rho^2}\right)\psi_K(\rho) = Q^2\psi_K(\rho) \tag{D.1}$$

where Q^2 is the total squared momentum and $\mathcal{L} = K + 3(A - 2)/2$ with hypermomentum K and ρ is the hyperradius. The hyper-radial eigensolutions of this Hamiltonian are

$$\psi_K(\rho) = \sqrt{Q\rho}J_{\mathcal{L}+\frac{1}{2}}(Q\rho). \tag{D.2}$$

With the Dirichlet boundary condition at $\rho = L$, QL become a zero of the spherical Bessel function $J_{\mathcal{L}+\frac{1}{2}}$. For i^{th} zero, we denote as $X_{i,\mathcal{L}}$ and compute the total square momentum as

$$Q_{i,n}^2 = \frac{X_{i,\mathcal{L}}^2}{L^2}. \tag{D.3}$$

The next step is to compute the eigenvalue of the kinetic energy operator in NCSM basis. We use the hyperspherical basis to avoid the computational requirement in computing the eigenvalues of kinetic energy operator. The kinetic energy matrix elements is tridiagonal as

$$\langle nK\gamma| \hat{T}_{NCSM} |n'K'\gamma'\rangle = \frac{\hbar\omega}{2}\delta_{KK'}\delta_{\gamma\gamma'}\left[\left(2n+\mathcal{L}+\frac{3}{2}\right)\delta_{nn'}\right.$$

$$\left. - \sqrt{(n+1)\left(n+\mathcal{L}+\frac{3}{2}\right)}\delta_{n+1,n'}\right], \tag{D.4}$$

and we compute the eigenvalues of the kinetic energy operator. The hyperspherical basis states $|nK\gamma\rangle$ collect the principle quantum number n, hypermomentum K and other quantum numbers characterizing the hyperspherical functions.

By comparing the lowest kinetic energy eigenstate in the hyper-radial well and the first eigenstate in the NCSM basis, the intrinsic IR length scales of the NCSM basis can be calculated through a relation

$$L_{eff} = b\sqrt{\frac{X_{1,\mathcal{L}}^2}{T_{1,\mathcal{L}}(N_{max}^{tot})}} = b\tilde{N}_{eff}, \tag{D.5}$$

with the effective angular momentum

$$\mathcal{L} = K_{min} + 3(A-2)/2, \tag{D.6}$$

where K_{min} is minimum hypermomentum, b is HO length, $\left(\frac{X_{1,\mathcal{L}}}{L}\right)^2$ is the lowest total squared momentum $Q_{1,n}^2$ of hyper-radial infinite square well, $X_{1,\mathcal{L}}$ is a zero of the spherical Bessel function $J_{\mathcal{L}+\frac{1}{2}}$. $\tilde{N}_{eff}$ depends on the number of particles and the model space truncation. More details can be found in Ref. (Wendt et al., 2015). The resulting IR length scales L_{eff} for corresponding hypernuclei are presented in Table D.1.

Table D.1 Effective $\tilde{N}_{eff}$ and IR length $L_{eff} = b\tilde{N}_{eff}$ for NCSM at $\Lambda_{UV} = 1200$ MeV for three- and four-body systems.

$N_{\max}^{tot}$	A=3			A=4		
	$\hbar\omega$	$\tilde{N}_{eff}$	L_{eff}	$\hbar\omega$	$\tilde{N}_{eff}$	L_{eff}
2	116.2995	3.6314	2.1685	99.0849	3.9343	2.5453
4	88.2357	4.1691	2.8582	77.4332	4.4504	3.2570
6	71.3360	4.6367	3.5354	63.8666	4.9004	3.9488
8	59.9587	5.0576	4.2062	54.4669	5.3064	4.6303
10	51.7498	5.4439	4.8734	47.5343	5.6802	5.3056
12	45.5368	5.8034	5.5384	42.1955	6.0288	5.9769
14	40.6659	6.1412	6.2017	37.9506	6.3571	6.6455
16	36.7421	6.4608	6.8640	34.4911	6.6683	7.3120
18	33.5125	6.7649	7.5255	31.6155	6.9649	7.9771
20	30.8070	7.0557	8.1864	29.1863	7.2490	8.6410
22	28.5073	7.3348	8.8468	27.1063	7.5220	9.3041
24	26.5281	7.6035	9.5069	25.3049	7.7851	9.9664
26	24.8065	7.8629	10.1666	23.7293	8.0394	10.6282
28	23.2954	8.1139	10.8261	22.3393	8.2858	11.2895
30	21.9581	8.3574	11.4855	21.1038	8.5248	11.9504
32	20.7664	8.5938	12.1446			
34	19.6975	8.8239	12.8036			
36	18.7335	9.0481	13.4625			
38	17.8595	9.2668	14.1213			
40	17.0636	9.4805	14.7799			
42	16.3357	9.6894	15.4385			
44	15.6673	9.8939	16.0971			
46	15.0517	10.0943	16.7556			
48	14.4826	10.2907	17.4140			
50	13.9550	10.4834	18.0723			
52	13.4645	10.6726	18.7307			
54	13.0074	10.8586	19.3890			
56	12.5802	11.0414	20.0472			

Table D.1 – (continued)

$N_{\max}^{tot}$	A=3			A=4		
	$\hbar\omega$	$\tilde{N}_{eff}$	L_{eff}	$\hbar\omega$	$\tilde{N}_{eff}$	L_{eff}
58	12.1803	11.2212	20.7055			
60	11.8051	11.3981	21.3637			
62	11.4522	11.5724	22.0218			
64	11.1199	11.7440	22.6800			
66	10.8063	11.9132	23.3381			
68	10.5099	12.0799	23.9962			
70	10.2294	12.2445	24.6543			
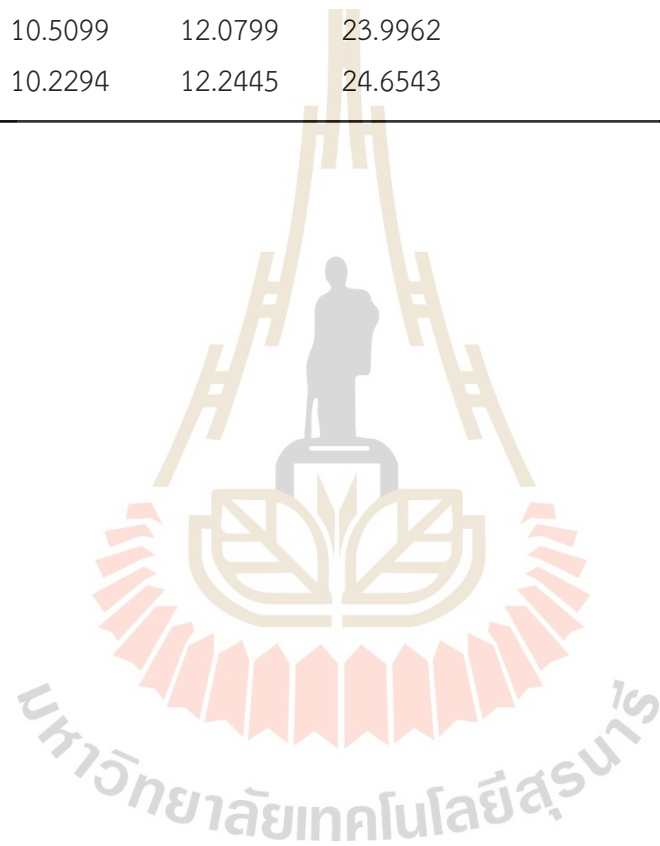
APPENDIX E

KINETIC ENERGY AND HAMILTONIAN

We express the kinetic energy operator $\widehat{T}$ needed for computing kinetic energy matrix elements of the Λnn system using hyperspherical harmonic basis when the finite Hamiltonian matrix is extended to the continuum state.

$$\widehat{T} = -\frac{\hbar^2}{2\mu_1 2}\vec{\nabla}_{x_{12}}^2 - \frac{\hbar^2}{2\mu_3}\vec{\nabla}_{x_3}^2,$$ (E.1)

where

$$\vec{x_{12}} = \vec{r}_1 - \vec{r}_2, \quad \vec{x_3} = \vec{r}_3 - \frac{m_1\vec{r}_1 + m_2\vec{r}_2}{m_1 + m_2}.$$ (E.2)

We may redefine the Jacobi coordinates,

$$\vec{X}_{12} = \sqrt{\frac{\mu_{12}}{m}}\vec{x}_{12},$$

$$\vec{X}_3 = \sqrt{\frac{\mu_3}{m}}\vec{x}_3,$$ (E.3)

to rewrite the kinetic energy term

$$T = -\frac{\hbar^2}{2m}\vec{\nabla}_{X_{12}}^2 - \frac{\hbar^2}{2m}\vec{\nabla}_{X_3}^2 = -\frac{\hbar^2}{2m}\vec{\nabla}_\rho^2$$ (E.4)

with

$$\vec{\rho} = \{\vec{X}_{12}, \vec{X}_3\}$$ (E.5)

Corresponding, one can define a hyperspherical oscillator,

$$H = -\frac{\hbar^2}{2m}\vec{\nabla}_\rho^2 + \frac{1}{2}m\omega^2\rho^2$$ (E.6)

APPENDIX F

HYPERSPHERICAL HARMONICS

Within HH approach, the total wavefunction is expanded in an infinite series over the hyperspherical harmonics as

$$\Psi = \sum_\mu \rho^{-5/2} u_{\kappa K}(E, \rho) \mathcal{Y}_\Gamma^{KLSJT}(\Omega_5, \vec{\chi}),$$

(F.1)

where $u_{\kappa K}$ is the hyperradial wavefunction and it can be expanded in hyperradial oscillator function series

$$u_K(E, \rho) = \sum_{\kappa=0}^{\infty} a_{\kappa K}(E) \mathcal{R}_{\kappa K}(\rho).$$

(F.2)

The hyperspherical harmonics spin-isospin function is formally defined as

$$
\begin{aligned}
\mathcal{Y}_\Gamma^{KLSJT}(\Omega_5, \vec{\chi}) &\equiv \mathcal{Y}_{K,l_1,l_2}^{m_1,m_2}(\Omega_5) \chi_s(\sigma) \chi_t(\tau) \\
&= P_K^{l_1,l_2}(\beta) \mathcal{Y}_{l_1 l_2}^{m_1,m_2}(\widehat{\xi}_1, \widehat{\xi}_2) \chi_s(\sigma) \chi_t(\tau) \\
&= P_K^{l_1,l_2}(\beta) \left\{ \left[Y_{l_1}^{m_1}(\widehat{\xi}_1) Y_{l_2}^{m_2}(\widehat{\xi}_2) \right]_{LM} [s_1 s_2]_S \right\}_{J J_z} \\
&\quad \times [t_1 t_2]_{T T_z},
\end{aligned}
$$

(F.3)

where $\vec{\chi}$ is the spin-isospin coordinate, $P_n^{\alpha,\nu}(x)$ is the hyper angle function and $Y_{lm}(\widehat{x})$ is the spherical harmonic. The hyperspherical harmonics have the following orthonormal relation:

$$\int \mathcal{Y}_{K,l_1',l_2'}^{m_1'm_2'}{}^*(\Omega_5)\mathcal{Y}_{K,l_1,l_2}^{m_1,m_2}(\Omega_5)d\Omega = \int_0^{\pi/2} P_K^{l_1,l_2}(\beta)P_K^{l_1,l_2}(\beta)\sin^2(\beta)$$

$$\times \cos^2(\beta)\mathrm{d}\beta$$

$$\times \int_0^{\pi}\int_0^{2\pi} Y_{l_1}^{m_1}{}^*(\widehat{\xi_1})Y_{l_1}^{m_1}(\widehat{\xi_1})$$

$$\times \sin\theta_1\mathrm{d}\,\theta_1\mathrm{d}\,\phi_1$$

$$\times \int_0^{\pi}\int_0^{2\pi} Y_{l_2}^{m_2}{}^*(\widehat{\xi_2})Y_{l_2}^{m_2}(\widehat{\xi_2})$$

$$\times \sin\theta_2\mathrm{d}\,\theta_2\mathrm{d}\,\phi_2$$

$$= \delta_{KK'}\delta_{l_1l_1'}\delta_{l_2l_2'}\delta_{m_1m_1'}\delta_{m_2m_2'},$$

(F.4)

where $\delta_{jj'}$ is the Kronecker delta and K is the grand angular momentum (hyper-momentum). The " $*$ means complex conjugate.

CURRICULUM VITAE

NAME: Thiri Yadanar Htun **GENDER**: Female

NATIONALITY: Myanmar **DATE OF BIRTH**: February 19, 1988

EDUCATIONS:

- M. Res. Department of Physics, Mandalay University, Mandalay, Myanmar, 2013.

- M. Sc. Department of Physics, Mandalay University, Mandalay, Myanmar, 2012.

- B. Sc. Department of Physics, Yadanarbon University, Mandalay, Myanmar, 2009.

AWARDS during PhD study:

[1] Award of Siam Physics Congress in Thailand (SPC 2018)
(Best presentation award together with another three competitors from SUT)

[2] Prize of Strangeness Nuclear Physics School in Japan for excellent presentation in the young researcher' session (2020)
(Incentive prize together with another five Japanese competitors)

PUBLICATIONS

[1] T. Y. Htun, D. Gazda, C. Forssén, Y. Yan, **"Systematic Nuclear Uncertainties in the Hypertriton System"**. Few-Body Syst **62,** 94 (2021). https://doi.org/10.1007/s00601-021-01675-4